TECHNISCHE UNIVERSITÄT MÜNCHEN

Fakultät für Chemie und Medizin

Lehrstuhl für Pharmazeutische Radiochemie

Development of Diagnostic and Therapeutic Radiopharmaceuticals targeting the Chemokine Receptor 4

Andreas Johannes Poschenrieder

Vollständiger Abdruck der von der Fakultät für Chemie der Technischen Universität München zur Erlangung des akademischen Grades eines

Doktors der Naturwissenschaften (Dr. rer. nat)

genehmigten Dissertation.

Vorsitzender: Prof. Dr. Dr. h.c. Horst Kessler

Prüfer der Dissertation:

1. Prof. Dr. Hans-Jürgen Wester
2. Prof. Dr. Klemens Scheidhauer

Die Dissertation wurde am 19.06.2017 bei der Technischen Universität München eingereicht und durch die Fakultät für Chemie am 28.09.2017 angenommen.

Für meine Eltern Elisabeth und Gottfried

Science knows no country, because knowledge belongs to humanity, and is the torch which illuminates the world.

Louis Pasteur

Die vorliegende Arbeit wurde im Zeitraum von Mai 2013 bis Juli 2016 in der Fakultät für Chemie am Lehrstuhl für Pharmazeutische Radiochemie der Technischen Universität München unter der Leitung von Prof. Dr. Hans-Jürgen Wester angefertigt.

Acknowledgement

Meinem Doktorvater, Herrn **Prof. Dr. Hans-Jürgen Wester**, danke ich für die äußerst interessante Themenstellung und die großartige Möglichkeit den Prozess der Radiopharmakaentwicklung von der einzelnen Aminosäure bis zur Anwendung des markierten Peptids im Menschen gestalten zu können. Ich bedanke mich vor allem für die kompetente Unterstützung und sein Vertrauen, das er mir entgegengebracht hat. Des Weiteren bedanke ich mich, dass ich die Möglichkeit hatte Vorlesungen zu halten, sowie Praktika und Bachelorarbeiten zu betreuen.

Ein besonderer Dank gebührt **Frau PD Dr. Margret Schottelius** für Ihre stets uneingeschränkte Unterstützung als Projektleiterin, auch in Situationen, in denen Sie selbst den Kopf über Wasser halten musste. Ich danke Ihr für Ihre aufmunternde und freundliche Art sowie alle hilfreichen Diskussionen.

Herzlichen Dank an Herrn **Prof. Dr. Klemens Scheidhauer** und an alle Mitarbeiter der Nuklearmedizin des Klinikum rechts der Isar, besonders auch an **Prof. Dr. Markus Schwaiger** für die stets gute Zusammenarbeit und **Christian Hundshammer, Dr. Benedikt Feuerecker, Nahid Yusufi, Dr. Franz Schilling** und **Stephan Düwel** für die gute und lustige Zeit in der „Denkzelle“.

Der **International Graduate School of Science and Engineering (IGSSE)** der Technischen Universität München, besonders der Unterstützung durch **Dr. Tobias Bidon**, danke ich für die großzügige finanzielle Unterstützung sowie für die Möglichkeit Weiterbildungen und einen spannenden Forschungsaufenthalt in Barcelona absolviert haben zu können. Für eine unvergessliche Zeit in Barcelona bedanke ich mich bei **Dr. Carles Mas-Moruno** und seinem Team mit **Dr. Roberta Fraioli, Dr. Giuseppe Sconti, Erica Roitero, Mireia Hoyos** und **Romain Schieber** sowie bei **Jing Jang, Miquel Turón, Jose Tarrago und Dr. Quentin Flamant**. Des Weiteren gilt mein Dank der IGSSE, da Sie eine beachtenswerte Kooperation mit **Prof. Dr. Horst Kessler** ermöglichte, die den Meinungsaustausch förderte und interessante Projektmeetings herbeiführte. Besonders danke ich **Dr. Tobias Kapp** für die gute Zusammenarbeit und die angenehme Zeit in Raithenhaslach.

Ein ganz spezieller Dank gilt **Dr. Martina Wirtz, PD. Dr. Johannes Notni, Dr. Behrooz Yousefi, Stephanie Robu**, **Theresa Osl, Alexander Schmidt, Dr. Frauke Hoffmann** sowie **Monika Beschorner** und **Sven Hintze** für eine unvergessliche Zeit im Labor und auf der Wies’n. Ebenso bedanke ich mich bei **Mathias Konrad**, **Daniel Di Carlo** und

Shalini Chopra, die mir den Laboralltag verschönert haben.

Vielen Dank an **Dr. Jakub Šimeček, Alexander Wurzer**, **Thomas Günther** und **Veronika Felber** sowie an meine Bacheloranden und Praktikanten für die Bereicherung und Unterstützung im Labor, sowie an **Michael Herz** für die Bereitstellung von ^{18}F und **Sybille Reder, Markus Mittelhäuser** und **Dr. Roswitha Beck** für die Unterstützung am Tiermodell.

Für die großartige gegenseitige Motivation während des Doktorstudiums bedanke ich mich bei **Dr. Julia Romic-Pickl. Natasha Bobrowski-Khoury** danke ich für ihre ständige Hilfsbereitschaft.

Herzlich möchte ich mich an dieser Stelle bei meiner Freundin **Gabriele Abel** für ihr Vertrauen und ihre liebevolle Unterstützung bedanken, die sie mir immer entgegengebracht hat.

Ein besonderer Dank gilt meiner Schwester **Sonja Poschenrieder** für ihre immer aufmunternde und erfrischende Art und insbesondere **meinen Eltern**, die mich vor, während, und nach dem Studium bis zum Abschluss der Promotion uneingeschränkt in jeglicher Form unterstützt haben.

List of Publications

Journal Contributions

Work on the presented PhD thesis resulted in the following publications:

1. **Poschenrieder A**, Schottelius M*, Osl T, Schwaiger M, Wester H-J. [^{64}Cu]NOTA-pentixather enables high resolution PET imaging of CXCR4 expression in a preclinical lymphoma model. EJNMMI Radiopharmacy and Chemistry. 2017;2:2.

2. Hyafil F*, Pelisek J, Laitinen I, Schottelius M, Mohring M, Döring Y, Van der Vorst E, Kallmayer M, Steiger K, **Poschenrieder A**, et al., Imaging the cytokine receptor CXCR4 in atherosclerotic plaques with the radiotracer [^{68}Ga]pentixafor for positron emission tomography. J. Nucl. Med. 2017;58(3):499-506. **Highlighted on cover**

3. **Poschenrieder A***, Schottelius M, Schwaiger M, Wester H-J. Preclinical evaluation of [^{68}Ga]NOTA-pentixafor for PET imaging of CXCR4 expression *in vivo* - a comparison to [^{68}Ga]pentixafor. EJNMMIR. 2016;6(1):1-5.

4. Schottelius M*, Osl T, **Poschenrieder A**, Hoffmann F, Beykan S, Hänscheid H, Franke K, et al., [^{177}Lu]pentixather: comprehensive preclinical evaluation of a first CXCR4-directed endoradiotherapeutic agent. Theranostics. 2017;7(9):2350-2362.

5. **Poschenrieder A***, Schottelius M, Schwaiger M, Kessler H, Wester H-J. The influence of different metal-chelate conjugates of pentixafor on the CXCR4 affinity. EJNMMI research. 2016;6(1):1-8.

6. **Poschenrieder A***, Osl, T, Schottelius, M, Hoffmann, F, Wirtz, M, Schwaiger, M, and Wester, H.J.. First ^{18}F-labeled pentixafor-based imaging agent for PET imaging of CXCR4-expression *in vivo*. Tomography. 2016;2(2):85-93. **Highlighted on cover**

7. Herrmann K*, Schottelius M, Lapa C, Osl T, **Poschenrieder A**, Haenscheid H et al. First-in-Human Experience of CXCR4-Directed Endoradiotherapy with ^{177}Lu and ^{90}Y-labeled Pentixather in Advanced-Stage Multiple Myeloma with Extensive Intra- and Extramedullary Disease. J Nucl Med. 2016;57(2):248-51.

8. Schottelius M*, Konrad M, Osl T, **Poschenrieder A**, Wester H-J. An optimized strategy for the mild and efficient solution phase iodination of tyrosine residues in bioactive peptides. Tetrahedron Lett. 2015;56(47):6602-5.

Conference Contributions

Work on presented PhD thesis resulted in the following conference oral presentations:

1. **Poschenrieder A**, Schottelius M, Weineisen M, Felber V, Kiwus C, Osl T, Schwaiger M, Wester HJ, First ^{18}F-labeled pentixafor-based imaging agent for high-contrast PET imaging of CXCR4-expression *in vivo*. Nuklearmedizin. 2015; 54, A15, V24

2. Lapa C, Knop S, Schirbel A, (…), **Poschenrieder A**, et al. First in man experience of CXCR4-directed endoradiotherapy with ^{177}Lu- and ^{90}Y-labelled Pentixather in multiple myeloma patients. Journal of Nuclear Medicine. 2015;56:14.

3. Schottelius M, Osl T, **Poschenrieder A**, et al. [^{177}Lu]pentixather: preclinical and first patient results with a highly promising CXCR4-directed endoradiotherapeutic agent. Journal of Nuclear Medicine. 2015;56:339.

Work on the presented PhD thesis resulted in the following patent:

Wester HJ, Schottelius M, Osl T, **Poschenrieder A**, Willibald M. Modified cyclopentapeptides and uses thereof. EP2014/061875, 2015.

English Abstract

The chemokine receptor 4 (CXCR4) and its only ligand CXC chemokine ligand 12 (CXCL12) are fundamentally involved in physiological processes and, amongst other diseases, also in tumor proliferation and tissue repair after myocardial infarction. Considering the fact that cancer is the second leading cause of death in developed countries, being only surpassed by cardiovascular diseases, the objective of the presented thesis was the development of diagnostic and therapeutic radiopharmaceuticals targeting CXCR4.

The thesis by publication covers four first author articles and four further publications with co-authorship, respectively. The first publication deals with the synthesis of CXCR4-targeting pentixafor-based cyclopentapeptides and their evaluation in terms of their CXCR4 affinity. Two new conjugates with an improved affinity compared to the parental compound [^{68}Ga]pentixafor have been identified.

In the second publication, [^{68}Ga]NOTA-pentixafor, identified as the compound with the highest CXCR4 affinity in the previous study, was evaluated as potential positron emission tomography (PET) tracer for CXCR4 expression *in vivo* and compared to [^{68}Ga]pentixafor.

The third publication shows the synthesis and preclinical evaluation of the first ^{18}F-labeled pentixafor derivative for PET imaging of CXCR4 *in vivo*. Both *in vitro* and *in vivo* CXCR4 targeting characteristics of [^{18}F]AlF-NOTA-pentixather are discussed and compared to [^{68}Ga]pentixafor.

The fourth publication reports on the synthesis and evaluation of ^{64}Cu-labeled NOTA-Pentixather in a preclinical lymphoma model. In the manuscript, a detailed investigation on the tracer stability *in vitro* and *in vivo* as well as biodistribution studies and small animal PET/CT are presented.

The publications with co-authership include investigations of [^{68}Ga]pentixafor as PET imaging agent for CXCR4 expression in atherosclerothic plaques, a novel synthesis procedure for the tyrosine iodination in bioactive peptides, and the comprehensive preclinical investigation of [^{177}Lu]pentixather as a first CXCR4-directed endoradiotherapeutic agent. In a further manuscript, the first clinical application of [^{177}Lu/^{90}Y]pentixather in patients with advanced stage multiple myeloma is presented.

Deutsches Abstract

Zusammen mit seinem einzigen endogenen Liganden CXCL12 ist der Chemokinrezeptor 4 (CXCR4) essentiell an physiologischen Prozessen beteiligt. Ebenso ist er, neben anderen Krankheiten, ein fundamentaler Bestandteil der Onkologie und dem Heilprozess nach dem Myokardinfarkt. Weil Krebs und kardiovaskuläre Erkrankungen die häufigsten Todesursachen in Industrieländern sind und die CXCR4/CXCL12 Achse maßgeblich an diesen Krankheiten beteiligt ist, war es Ziel der Arbeit, diagnostische und therapeutische Radiopharmaka für den CXCR4 Rezeptor zu entwickeln.

Die kumulative Dissertation setzt sich aus jeweils vier Erstautoren-publikationen und vier weiteren Publikationen als Koautor zusammen. In der ersten Publikation wird die Synthese zahlreicher Pentixafor-basierter Cyclopentapeptide und deren CXCR4 Affinitätsevaluierung beschrieben. Es wurden zwei Peptide mit einer höheren Affinität zu CXCR4 im Vergleich zu [^{68}Ga]pentixafor gefunden.

Da [^{68}Ga]NOTA-pentixafor in der vorherigen Studie als das CXCR4 affinste Peptid identifiziert wurde, wurde es in einer zweiten Publikation präklinisch als potentieller Tracer für die PET Bildgebung evaluiert und mit [^{68}Ga]pentixafor verglichen.

In der dritten Publikation wird die Synthese und Evaluation von [^{18}F]AlF-NOTA-pentixather im präklinischen Lymphom Modell zur PET Bildgebung von CXCR4 Expression *in vivo* beschrieben. Mit Bezug auf [^{68}Ga]pentixafor werden die CXCR4 Bindungseigenschaften des ^{18}F-markierten Tracers sowohl *in vitro* als auch *in vivo* diskutiert.

In der vierten Studie wird NOTA-pentixather mit ^{64}Cu markiert und im präklinischen Lymphom Modell als PET Tracer evaluiert. Im Manuskript werden neben Stabilitätsuntersuchungen und *in vitro* und *in vivo* CXCR4 Bindungseigenschaften auch Biodistributionsstudien und Kleintier-PET diskutiert.

Die Koautorenpublikationen beinhalten Studien an [^{68}Ga]pentixafor zur PET Bildgebung von CXCR4 in Atheroskleroseplaques, eine neue Synthese zur Iodierung von Tyrosinen in bioaktiven Peptiden und eine detaillierte präklinische Untersuchung von [^{177}Lu]pentixather als ersten Tracer für CXCR4-gerichtete Endoradiotherapie. In einem weiteren Manuskript wird die erste klinische Anwendung von [^{177}Lu/^{90}Y]pentixather in Patienten mit Multiplen Myelom im fortgeschittenen Stadium dargelegt.

List of Abbreviations

AMB	4-(aminomethyl)benzoic acid
AML	Acute myeloid leukemia
CLL	Chronic lymphocytic leukemia
CUP	Cancer of unknown primary origin
CXCL12	CXC chemokine ligand 12
CXCR4	Chemokine receptor 4
DFO	Desferrioxamine
DOTA	1,4,7,10-tetraazacyclododecane-1,4,7,10-tetraacetic acid
DOTAGA	1,4,7,10-tetraazacyclododecane,1-(glutaric acid)-4,7,10-triacetic acid
DTPA	Diethylenetriaminepentaacetic acid
EDTA	Ethylenediaminetetraacetic acid
FDG	2-fluoro-2-deoxyglucose
GPCR	G protein-coupled receptor
HIV-1	Human immunodeficiency virus-1
ID/g	Injected dose per gram tissue
LET	Linear energy transfer
MIP	Maximum intensity projection
MM	Multiple myeloma
NCS-MP-NODA	2,2'-(7-(4-isothiocyanatobenzyl)-1,4,7-triazonane-1,4-diyl)diacetic acid
NHL	Non-Hodgkin lymphoma
NIS	N-iodosuccinimide
NODAGA	1,4,7-triazacyclononane,1-glutaric acid-4,7-acetic acid
NOTA	1,4,7-triazacyclononane-triacetic acid
p-SCN-Bn-DTPA	2-(4-isothiocyanatobenzyl)-diethylenetriamine pentaacetic acid
p.i.	Post injection
PET	Positron emission tomography
PMT	Photomultiplier tube
PRRT	Peptide receptor radionuclide therapy
RBC	Red blood cell
SCLC	Small cell lung cancer
SDF-1	Stromal cell-derived factor 1
SPECT	Single photon emission computed tomography
SUV	Standardized uptake value
TETA	1,4,8,11-tetraaza-cyclododecane-1,4,8,11-tetraacetic acid
TMH	Transmembrane helix

Table of Contents

I. Background

I.1 CXCR4/CXCL12 Axis in Physiology and Disease

The interaction between the chemokine receptor 4 (CXCR4) and its ligand CXC chemokine ligand 12 (CXCL12), also known as stromal cell-derived factor 1 (SDF-1), plays a pivotal role in physiology and is also involved in various states of pathology. In developed countries, cancer is the second leading cause of death, being only surpassed by cardiovascular diseases. The involvement of the CXCR4/CXCL12 axis in these diseases highlights the importance of CXCR4 as molecular target for tracer development. Developing diagnostic and therapeutic radiopharmaceuticals targeting CXCR4 aims towards better patient management and personalized medicine.

Activation of the G protein-coupled receptor (GPCR) CXCR4 by its only endogenous ligand CXCL12 initiates unique cell signaling cascades and stimulates cell migration (Figure 1). In physiology, the CXCR4/CXCL12 axis regulates cell adhesion, proliferation and survival, as well as chemotaxis and the trafficking of leukocytes. Moreover, it is essential for the migration of progenitor cells during hematopoiesis, organogenesis, and tissue regeneration (*1-3*). Deficiency of the CXCR4 gene for instance, is lethal during embryogenesis as it leads to impaired organ development and defective cardiogenesis (*4,5*).

In pathology, CXCR4 plays a critical role in the human immunodeficiency virus-1 (HIV-1) entry into target cells, inflammation, and myocardial infarction. In oncology, CXCR4 is fundamentally involved in tumor growth and tissue specific metastasis to organs constitutively expressing CXCL12 such as the bone marrow, lungs, and liver (*6*). As illustrated in Figure 2, CXCL12 and CXCR4 receptor expression is increased in hypoxic regions of the tumor leading to enhanced tumor cell motility and invasiveness.

CXCR4 is overexpressed in more than 30 different tumor types including lymphoproliferative diseases such as non-Hodgkin lymphoma (NHL), Hodgkin lymphoma, multiple myeloma (MM), and chronic lymphocytic leukemia (CLL) but also brain, breast, pancreas, prostate, kidney, ovarian cancer, and melanoma (*7-12*). Physiological expression of CXCR4, which is highest in T-lymphocytes, B-lymphocytes, monocytes, macrophages, neutrophils, as well as endothelial and hematopoietic stem and progenitor cells in the bone marrow (*13,14*), is markedly lower than in tumors (*15*). Overexpression of CXCR4 on tumor cells and CXCL12 secretion in the tumor microenvironment results in enhanced stimulation of the CXCR4 receptor promoting proliferation, inhibiting apoptosis, and driving tumor growth.

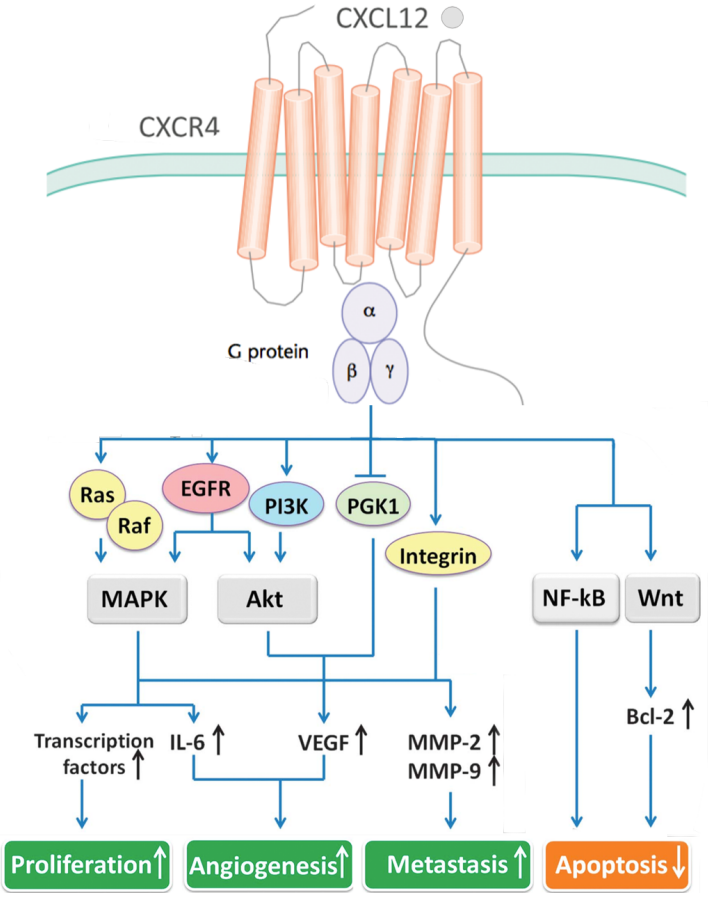

Figure 1: CXCR4/CXCL12 signaling pathway. Activation of the chemokine receptor CXCR4 suppresses apoptosis and promotes tumor proliferation, angiogenesis, and metastasis – modified image from (16).

More specifically, CXCL12 can induce CXCR4-positive cancer cells to secrete interleukin-8, macrophages to secrete epidermal growth factor, and stem cells to secrete vascular endothelial growth factor establishing a tumor-favorable microenvironment (*8,17*). The CXCR4/CXCL12 axis promotes tumor growth by neoangiogenesis i.e. through the recruitment of endothelial progenitor cells to sites of neovascularization in tumors (Figure 2). Increased CXCR4 expression in cancer cells is also significantly correlated with an aggressive phenotype (*13*), an increased risk of recurrence (*18*), and low overall and disease-free survival rates in various cancers (*19-21*).

Consequently, CXCR4 is not only a biomarker of immense value for non-invasive diagnostics, image guided therapy, and response monitoring, but also for disrupting CXCR4-dependent tumor-stroma interactions in order to impair tumor proliferation and metastasis and to increase sensitivity of tumor cells to anticancer therapies.

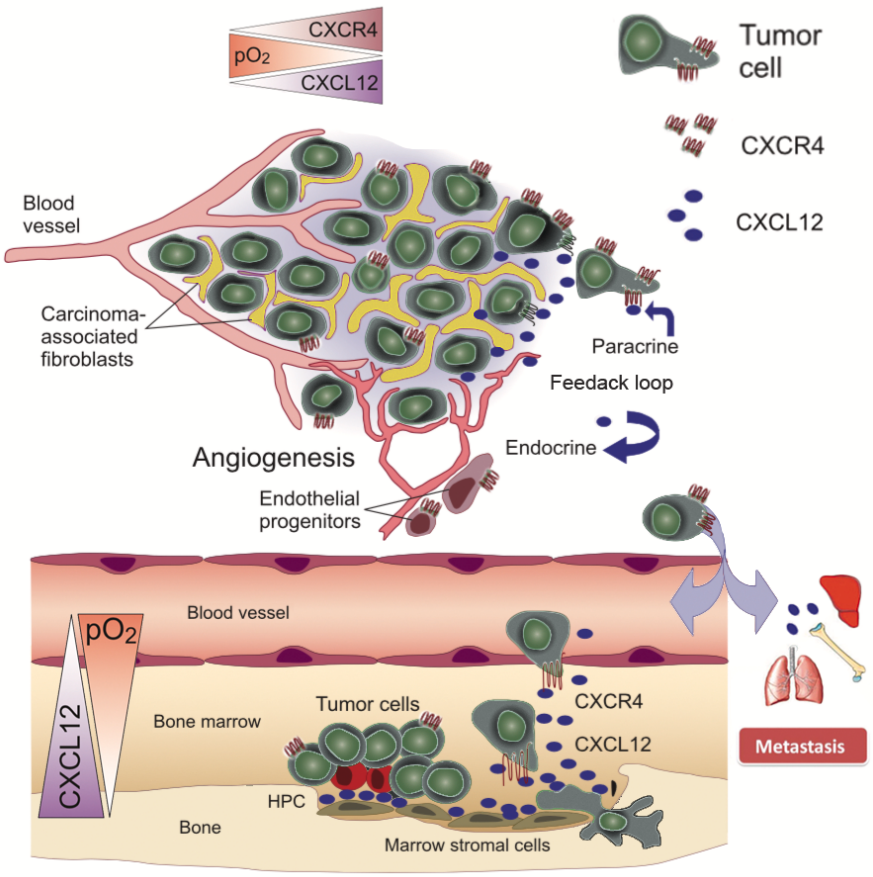

Figure 2: Schematic illustration of the CXCR4/CXCL12 axis promoting tumor growth by para and endocrine feedback loops and recruiting of endothelial progenitor cells which drive angiogenesis. CXCR4 and CXCL12 expression is upregulated in hypoxic tumors favoring tumor motility and distant tissue specific metastasis to sites of abundant levels of CXCL12 expression like in liver, lungs, bones, and bone marrow - modified image from (8).

I.2 Ligand-Receptor Interactions

Chemokine receptors are a family of seven transmembrane domain GPCRs and are designated CXCR1 through CXCR5, CCR1 through CCR11, XCR1, and CX3CR1, based on their specific preference for certain chemokines (*22*). CXCR4 is one of 19 known human chemokine receptors (*23*). Chemokines (*chemo*attractive cyto*kines*) can be segregated into two main subfamilies (CXC or CC) based on weather the two N-terminal conserved cysteines are separated by an intervening amino acid. Following activation of GPCRs, one or several heterotrimeric G proteins are activated by stimulation of guanosine diphosphate/guanosine triphosphate exchange which eventually triggers a specific signaling cascade (compare Figure 1). Recently determined crystal structures of CXCR4 with different ligands revealed structural features facilitating structure-function analyses and ligand discovery (*24*).

Many attempts, including molecular modeling studies, have been undertaken to identify the binding mode of CXCR4-targeting peptides (*25-28*). As illustrated in Figure 3, starting point for ligand development throughout this thesis was the scaffold of pentixafor, a potent CXCR4-targeting cyclic pentapeptide derived from FC131 (*cyclo*(-D-Tyr^1-Arg^2-Arg^3-2-Nal^4-Gly^5-) (Figure 3) (*29*). FC131 was designed by Fuji et al. by downsizing polyphemusin II, an antimicrobial peptide isolated from hemocytes of the American horseshoe crab *Limulus polyphemus* (*30-32*). FC131 contains the four most important (basic and aromatic) residues indispensable for CXCR4 affinity (Figure 3). Glycine was used for pentapeptide cyclization, which is associated with high stability towards enzymatic degradation and commonly low toxicity (*29,33*).

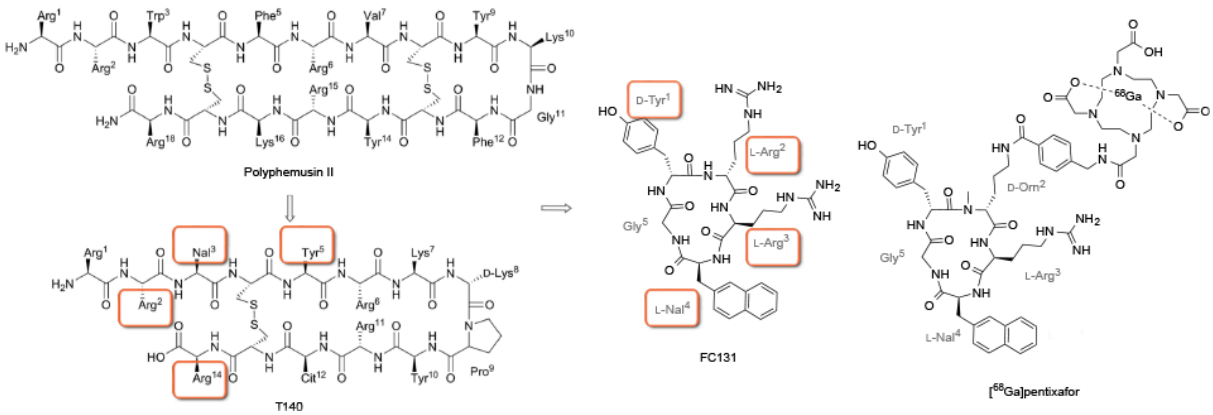

Figure 3: Chemical structures of CXCR4-targeting Polyphemusin II, T140, FC131, and [^{68}Ga]pentixafor. Amino acid residues that were highlighted are indispensable for receptor binding and were conserved during downsizing to the cyclic pentapeptides.

Since the extracellular surface of CXCR4 is mainly negatively charged (*24*), molecular recognition between FC131 and CXCR4 is presumably initiated by ionic interactions between the positively charged residues of the peptide and one or more negatively charged receptor residues (*34*). Upon receptor binding, the guanidino group of the Arg[3] side chain of FC131 protrudes in a tight binding pocket, being involved in a complex charge-assisted H-bond network with several receptor residues (His[113], Thr[117], and Asp[171], Figure 4) (*34*).

Ligand/receptor interaction studies of the cyclopentapeptide FC131 with CXCR4 also revealed that the lipophilic aromatic amino acid residue L-2-Nal[4] is buried in a well-defined hydrophobic subpocket in transmembrane helix (TMH) 5, which leaves the D-Tyr[1] and L-Arg[2] residues located on the opposite side near TMH 1 at the N-terminal fragment of CXCR4 partially solvent exposed (Figure 4) (*24,35*). While L-Arg[3] is essential for binding, position 2 is therefore more flexible towards modification. Hence, L-Arg[2] of FC131 was substituted by D-Orn and *N*-methylated for higher CXCR4 affinity. For covalent linkage of the chelator to the peptide, a number of spacers have been investigated (*36*) and 4-(aminomethyl)benzoic acid (AMB) proved highly suited regarding the CXCR4 affinity. As the chelator, 1,4,7,10-tetraazacyclododecane-1,4,7,10-tetraacetic acid (DOTA) was conjugated in order to create a radiopharmaceutical for potential diagnostic (positron emission tomography (PET), single photon emission computed tomography (SPECT)) and therapeutic purposes such as peptide receptor radionuclide therapy (PRRT) (*36,37*).

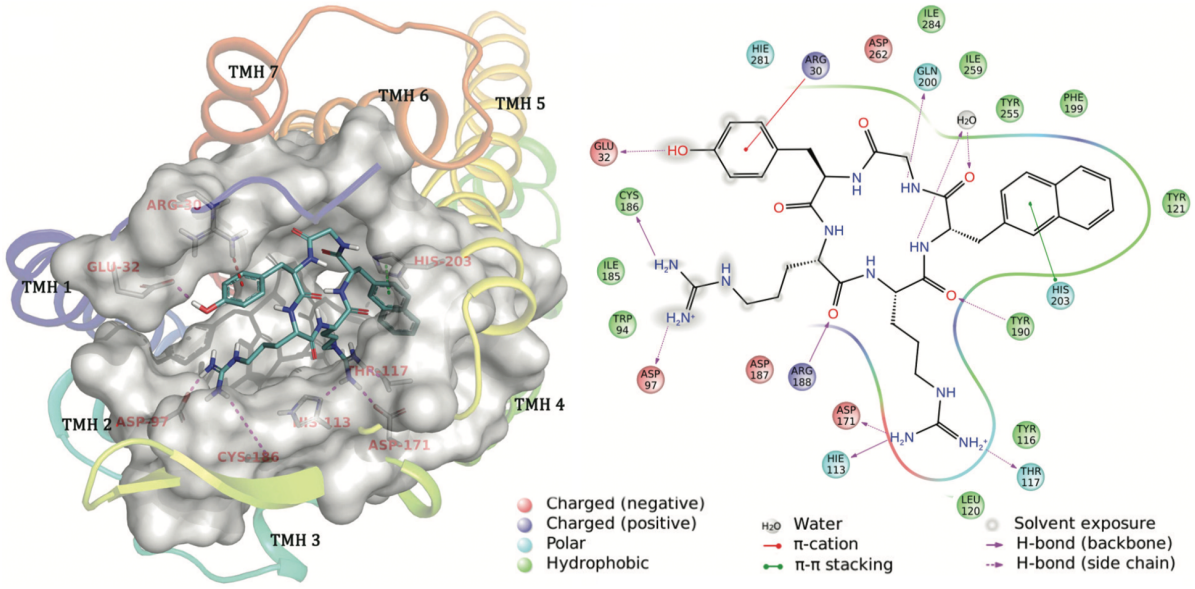

Figure 4: Proposed binding mode of the cyclopentapeptide FC131 with CXCR4. Seven transmembrane helices (TMH 1-7) and binding pocket (gray) with selected interactions (left); detailed molecular interactions of FC131 with CXCR4; Arg[2] and Tyr[1] are partially solvent exposed (indicated by water interaction, gray) (35).

I.3 CXCR4 Ligand Development

Before its discovery as a chemokine receptor, CXCR4 was identified to mediate entry of T cell line-tropic (T-tropic) HIV-1 strains (*38*), a process that could be inhibited by CXCL12 (*39*). The identification of CXCR4 as a co-receptor for HIV-1 entry triggered the development of CXCR4 antagonists such as potent synthetic CXCL12-analogs like the tetradecapeptide T140 (*40*), the bicyclam AMD3100 (*41,42*), and the peptide inhibitor ALX40-4C (*43*). Initial (phase I) clinical trials with AMD3100 to assess its antiviral efficacy in HIV-infected individuals started in 2000 (*41,44*). Until today, AMD3100 is the only CXCR4-targeting agent that has been approved by the Food and Drug Administration for autologous bone marrow transplantation in multiple myeloma (MM) and non-Hodgkin's lymphoma (NHL) (*45*).

Since the identification of the role of CXCR4 in the regulation of tissue specific metastasis in breast cancer (*7*) and its fundamental role in oncology, a number of (small-molecule based) CXCR4 inhibitors have been developed for therapeutic purposes, e.g. antagonizing CXCR4 with AMD3100 was shown to cause both decreased survival and proliferation and increased sensitivity to anticancer therapies *in vitro* and *in vivo* (*46,47*). Various CXCR4 inhibitors for therapeutic purposes have been reviewed in several publications (*48-55*). To overcome the currently unmet clinical need for non-invasive diagnostic imaging of CXCR4 expression, different imaging agents for the CXCR4 receptor have been developed.

The first radiolabeled probe for SPECT/PET imaging of CXCR4 expression *in vivo,* [^{125}I]CPCR4 was published by Koglin et al. in 2006 (*56*). In the same year, Hanaoka et al. developed a T140 derivative conjugated to diethylenetriaminepenta-acetic acid (DTPA) and radiolabeled with ^{111}In for SPECT imaging (*40*). The first ^{18}F-labeled CXCR4 PET imaging agent, [^{18}F]T140, has been developed by Jacobson et al in 2010 (*57*). Other important CXCR4 targeted imaging agents include AMD3100 (plerixafor)-based radioligands (*58-68*) that have been labeled with ^{64}Cu (*64-67,69*), ^{18}F (*70*), ^{11}C (*71*), and ^{68}Ga (*72*) and targeted peptides, including derivatives of T140 (*40,57,73-80*) and FC131 (*36,37,81-83*). Summaries of CXCR4-targeting probes have recently been reported in excellent reviews (*84-87*) and a detailed overview of CXCR4 targeting imaging probes for SPECT and PET are discussed in chapter I.7 and I.8, respectively.

Amongst CXCR4-directed imaging agents, [^{68}Ga]pentixafor (*36,37*) holds a unique position, because of its high affinity and selectivity to *h*CXCR4 but not to CXCR7 or *m*CXCR4, low unspecific binding, and adequate distribution profile accompanied by fast renal excretion. Combined with a favorable dosimetry (*88*), these characteristics paved the way for first currently ongoing clinical studies for high contrast PET imaging of CXCR4 expression in patients with lymphoproliferative diseases (*89*), acute myeloid leukemia (AML) (*90*), multiple

myeloma (*91,92*), adrenocortical cancer (*93*), glioblastoma (*94*), small cell lung cancer (SCLC) (*95*), and solid cancers (*96*). An overview of [^{68}Ga]pentixafor PET/CT imaging in different cancers (proof-of-concept) is shown in Figure 5. [^{68}Ga]pentixafor PET has also shown to be valuable for CXCR4 quantification in atherosclerosis (*97*) and after myocardial infarction (*98-101*).

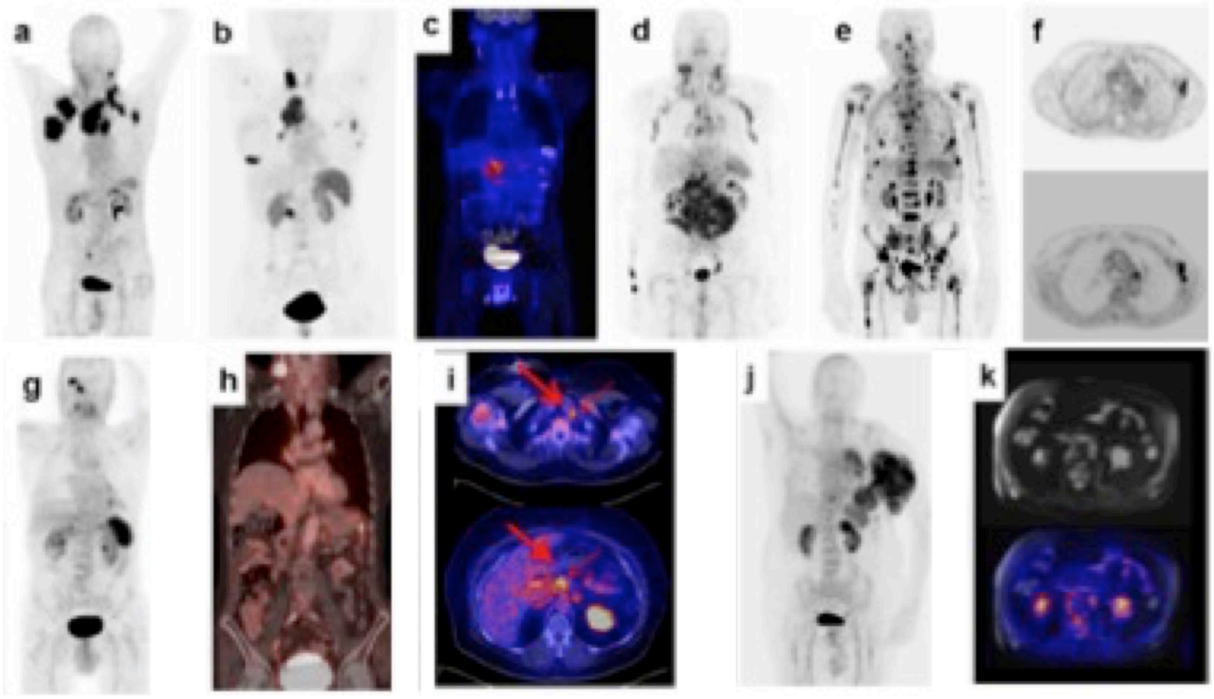

Figure 5: Imaging of CXCR4 receptor expression using [^{68}Ga]pentixafor PET/CT in patients: a) Mantle Cell Lymphoma, b) Cancer of unknown primary origin (CUP) (pancreas), c) Pancreatic Cancer, d) Chronic Lymphomcytic Leukemia (102), e) Myeloma (102), f) Breast Cancer (lower panel: 2-[^{18}F]fluoro-2-deoxyglucose *([^{18}F]FDG) PET), g and h) Small Cell Lung Cancer, i) Pancreatic Cancer, j) T-cell Lymphoma, k) Prostate Cancer - (103).*

I.4 Radiometals and Chelators

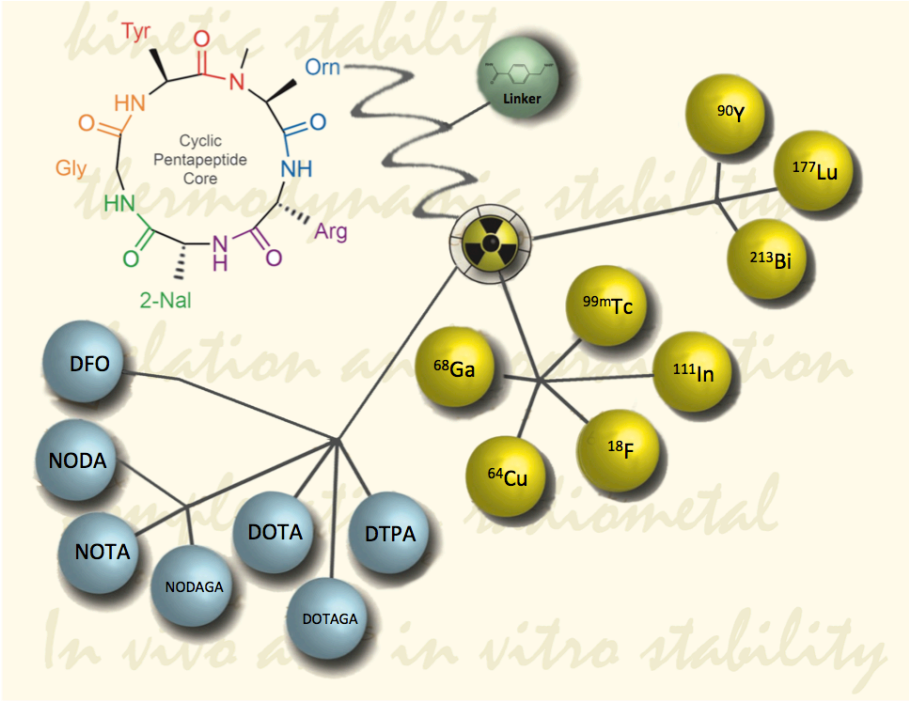

Figure 6: Schematic illustration of different radionuclide-chelators-conjugates covalently bound to the CXCR4-targeting pentapeptide core (cyclo(Gly-L-Nal-L-Arg-D-Orn-D-Tyr)) of pentixafor via a 4-(aminomethyl)benzoic acid (AMB) spacer.

As schematically illustrated in Figure 6, a radiopharmaceutical consists of four components, i) biomolecular vector, i.e. the cyclic pentapeptide core, ii) chelator, iii) radionuclide, and iv) covalent link between chelator and biomolecule. While chapter I.2 and I.3 focus on interactions of pentapeptides with the CXCR4 receptor and ligand development for CXCR4, chapter I.4 will briefly introduce selected radiometals and chelators in the context of radiopharmaceutical development. For a more detailed introduction, the interested reader is referred to excellent reviews on radiometals and their use in nuclear medicine (*104-109*).

Radiometals are radioactive isotopes and, depending on the decay properties, can be used for diagnostic imaging such as SPECT (e.g. ^{67}Ga, ^{99m}Tc, ^{111}In, ^{177}Lu), PET (e.g. ^{68}Ga, ^{64}Cu, ^{44}Sc, ^{86}Y, ^{89}Zr), but also targeted cancer therapy. While β-emitters of different energy (^{90}Y, ^{177}Lu) enable individualized targeting of tumors of a given size, α-emitters (e.g. ^{211}At, ^{213}Bi, ^{225}Ac) can be used for the targeted therapy of micrometastases. Decay properties of selected SPECT and PET radionuclides (Table 1 and 2, respectively) as well as radionuclides for targeted therapy can be found in Table 3.

Because of its physical decay properties, ^{18}F rapidly became the isotope of choice for PET imaging. Nevertheless, the half-life of ^{18}F and other isotopes, which are traditionally used for

PET imaging (e.g.^{15}O, ^{13}N, or ^{11}C), is often insufficient to meet the biological half-lives of macromolecular targeting agents such as peptides, antibodies, fragments, and oligonucleotides. Moreover, the radiochemistry with non-metallic isotopes often requires complex syntheses with conditions that are not compatible with sensitive biomolecular vectors.

Radiometals such as ^{89}Zr, ^{86}Y, ^{68}Ga, and ^{64}Cu have been investigated for PET imaging (*108*) and, with the exception of ^{68}Ga, they typically have longer half-lives compared to non-metallic nuclides such as ^{18}F or ^{11}C. Moreover, many bifunctional chelators are available for the complexation of the respective radiometal. Covalent linkage of the bifunctional chelator to the biological vector is straightforward, e.g. by activation of one of its carboxyl groups and subsequent reaction with a free amine of the biomolecule while labeling of the radionuclide is relatively fast and can be achieved under mild reaction conditions in aqueous solution. Figure 7 shows two major classes of bifunctional chelators i) acyclic chelators such as ethylenediaminetetraacetic acid (EDTA), DTPA, citrate, desferrioxamine (DFO), and ii) macrocyclic chelators (e.g. DOTA, 1,4,8,11-tetraaza-cyclododecane-1,4,8,11-tetraacetic acid (TETA), 1,4,7-triazacyclononane-triacetic acid (NOTA), sarcophagines).

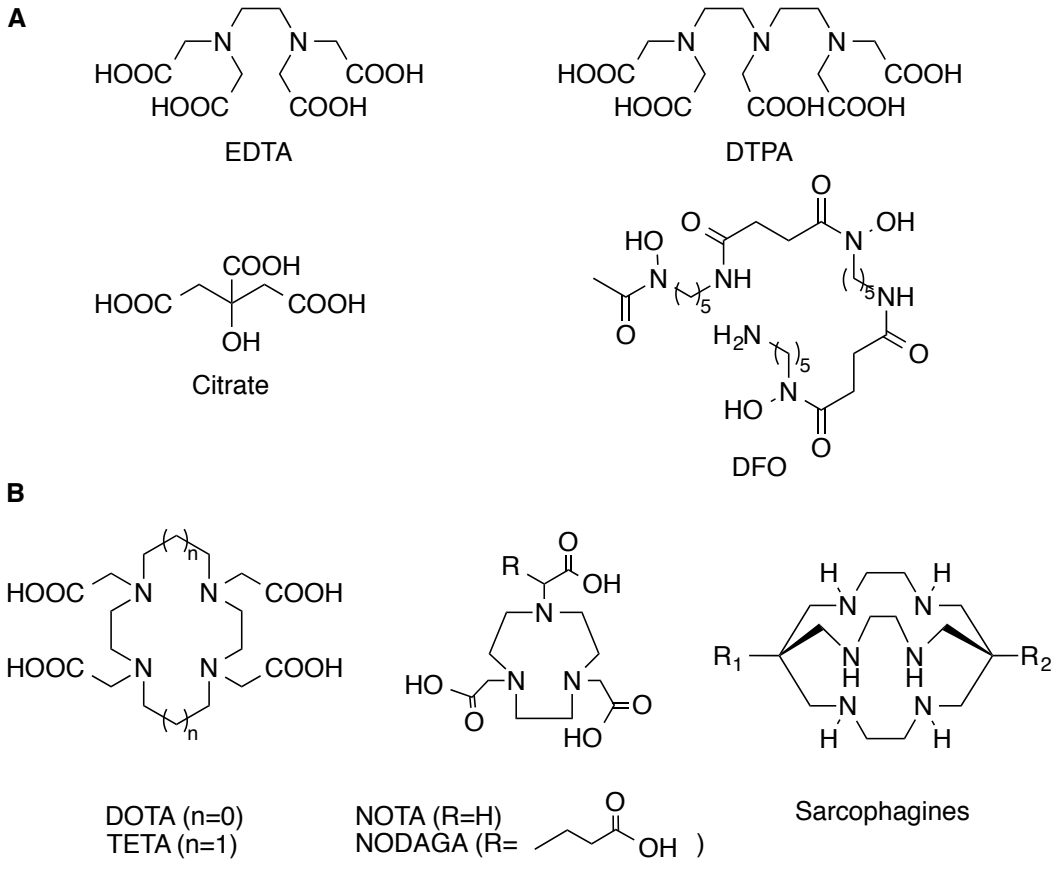

Figure 7: Selected acyclic (A) and macrocyclic chelators (B).

Compared to acyclic complexes, macrocyclic chelators show generally slower complexation kinetics but higher kinetically inertness, i.e. less transchelation of the radionuclide to metal-dependent enzymes (e.g. superoxide dismutase) or proteins (e.g. caeruloplasmin) in the case of Cu-labelled conjugates (*110-112*). The chelators depicted in Figure 7 are widely used for the complexation of different metals including, amongst others, Cu^{2+}, Ga^{3+}, Bi^{3+}, Lu^{3+}, and Zr^{4+} (*113,114*). ^{18}F is the most commonly used radionuclide for PET imaging and well known from its use in 2-[^{18}F]fluoro-2-deoxyglucose ([^{18}F]FDG). In order to evade challenging coupling reactions of ^{18}F to a carbon atom of the biological vector and to facilitate radiofluorination, NOTA and derivatives as well as other chelators have been used to capture the $Al^{18}F^{2+}$ complex (*115*) since fluorine forms a very stable bond with Al^{3+} (*116*).

Fundamentally, the main task of a chelator consists in the efficient chelation of the radionuclide as well as in being thermodynamically stable and kinetically inert in order to resist both transchelation to endogenous ligands (e.g. ceruloplasmin (*117*), superoxide dismutase (*111*), and transferrin (*118*)) and transmetallation by endogenous metal ions (e.g. Ca^{2+} or Zn^{2+}) *in vivo*. The choice of the correct chelator for a specific radionuclide in terms of donor atoms, coordination, and geometry is crucial for the stability of the conjugate since loss of the radiometal would result in unspecific activity accumulation, toxicity, and poor image quality.

I.5 SPECT Imaging

Image acquisition in SPECT utilizes γ-emitting isotopes, which, upon decay, emit a photon that is detected by a γ–camera (scintillation detectors, Anger cameras). In general, a radioactive tracer is injected and its distribution is thereafter monitored by rotation of often two or three camera heads around the patient at multiple angles (Figure 8). For anatomical information, SPECT is usually combined with CT.

The Anger camera consists of a single rectangular NaI(Tl) crystal optically coupled to an array of 30-100 photomultiplier tubes (PMTs) to the back face of the crystal (*119*). The primary mode of interaction of emitted photons with the atoms in the scintillation crystal is the photoelectric effect. For the crystal to emit light (scintillation photon) in the visible range, an alkali halide crystal, e.g. sodium iodide doped with thallium iodide (NaI(Tl)), is used. The scintillation photon (3-4 eV) is then converted into a measureable current (mA) by a photodetector. Usually PMTs are used as photodetectors to amplify the released photoelectrons to $>10^6$ after the initial scintillation photon stroke the photocathode of the PMT (*119*).

Most cameras consist of a ~10 mm thick crystal for optimum performance between 120 and 200 keV photons (*119*). ^{99m}Tc (141 keV) therefore offers almost ideal decay characteristics for NaI(Tl) crystals which show a detection efficiency >90% for 140 keV photons, (but less than 10% for 511 keV photons) (*119*). The favorable nuclide properties of ^{99m}Tc and its ready availability from the ^{99m}Mo/^{99m}Tc-generator make it the most widely used radionuclide for SPECT imaging (*120*). Other radionuclides for SPECT imaging are listed in Table 1.

In order to define the angle of incidence, physical collimators, usually made of lead, with specific holes (e.g. parallel or pinhole) are used to reject photons that travel in an oblique angle to the axes of the holes. Collimators therefore exhibit low geometric efficiencies, de-

Table 1: Physical decay properties of selected SPECT radioisotopes (*121*). EC: electron capture; IT: isomeric transition.

Isotope	Half-life	Decay	γ-energy [keV]
^{67}Ga	3.3 d	EC	93, 185, 300
^{99m}Tc	6.0 h	IT	141
^{111}In	2.8 d	EC	171, 245
^{123}I	13.2 h	EC	159, 529
^{201}Tl	73.1 h	EC	167, 135

fined as the percentage of detected to emitted photon, in the range of $1/10^4$, which limits the sensitivity of SPECT i.e., the ability to detect and record a higher percentage of the events (*122*). The origin of the photon coming from the patient is eventually determined by the location of the scintillation event on the crystal, which causes PMTs that are close to the event to produce a higher electrical current than distant PMTs (*119*). After conversion to a digital signal and image reconstruction a three-dimensional image of the radiotracer's distribution in the patient is created.

The overall sensitivity and resolution of the camera is determined by the thickness of the collimator and septa as well as the number of holes and the distance of the detector from the γ-source. Shorter collimators have been designed to reach higher sensitivity by rejection of a smaller portion of incident events. However the resolution is degraded by this approach and eventually there is a design compromise between sensitivity and resolution (*122*). Spatial resolutions of SPECT cameras are in the 8 - 12 mm range in clinical applications and spatial variations of radioactivity concentrations that are in close proximity down to 0.4 mm for preclinical scanners can be distinguished (*123*).

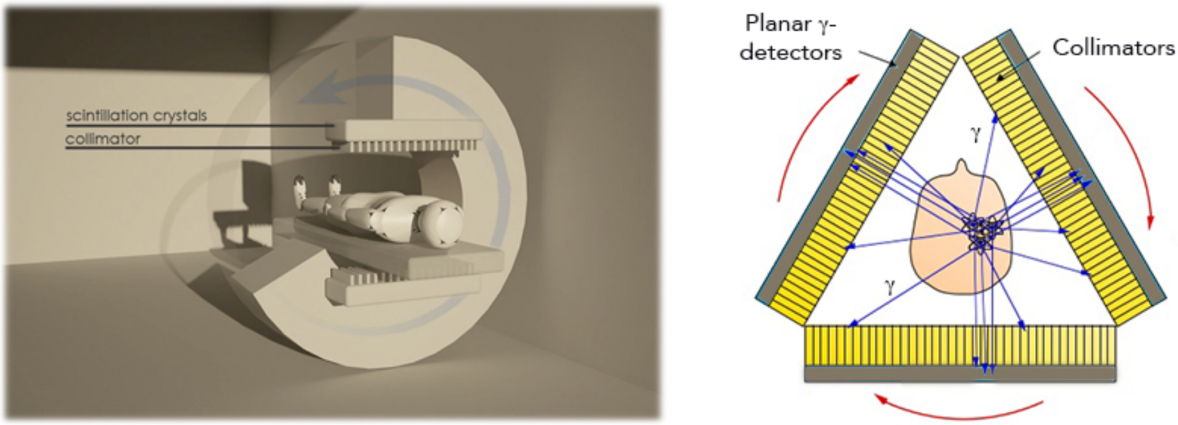

Figure 8: Principle of SPECT: a radioisotope decays by emission of γ rays which are detected by a γ-camera consisting of a collimator, scintillation crystal, light guide, array of PMTs and related electronics for image acquisition – modified image from (124).

I.6 PET Imaging

A PET scanner usually consists of a detector (scintillator coupled to PMTs), collimators (to define the field of view), signal processing electronics, coincidence circuit, a computer for data acquisition with reconstruction, display, and image analysis systems (*119*).

In the radioactive decay by positron emission, a proton in the nucleus is transformed into a neutron, a positron (β^+) and a neutrino (n). A selection of relevant positron emitting radioisotopes and decay properties is summarized in Table 2. Depending on the positron energy of the radionuclide, the emitted positron will travel a certain distance and expend its kinetic energy in collisions with the surrounding medium until its thermal energy allows combination with an electron to form a positronium (Figure 9). Upon positron-electron annihilation, their masses are converted to energy in form of two 511 keV photons, which are emitted from the same event, 180° apart. A PET scanner detects the photons almost simultaneously on the basis of the coincidence detection method with typical timing windows of 6-12 ns. In the time of flight mode, the exact location of the annihilation event (and not the point of positron emission) can be determined by measuring the difference in arrival time of the two annihilation photons at the opposite detectors. Mathematical algorithms like iterative approaches, e.g. ordered subset expectation maximization (OSEM), are used to reconstruct three-dimensional images from two-dimensional projections (*125*).

Compared to NaI(Tl) crystals in SPECT, e.g. bismuth germanate ($Bi_4Ge_3O_{12}$, BGO) crystals are used as scintillation crystal as they detects significantly more (80%) of the incident 511 keV photons (*119*). Since the size of the crystal determines spatial resolution, smaller crystals have been developed; they have been reduced from 5 mm to 1.5 mm for human scanners and to sizes of only 0.975 mm (*126,127*) for small animal µPET.

Table 2: Physical decay properties of selected positron emission radioisotopes with range of positrons in water (*128*).

Isotope	Half-life	Branching (β^+) in %	E_{max} [MeV]	R_{max} [mm]
^{11}C	20.4 min	99.8	0.960	4.2
^{13}N	10.0 min	99.8	1.199	5.5
^{15}O	2.0 min	99.9	1.732	8.4
^{18}F	109.7 min	96.9	0.634	2.4
^{64}Cu	12.7 h	17.5	0.653	2.5
^{68}Ga	67.8 min	89.9	1.899	9.2
^{89}Zr	78.8 h	22.7	0.902	3.8
^{124}I	100.2 h	22.7	2.138	10.0

To obtain quantitative data of the radiotracer uptake and tissue distribution, the projections need to be corrected before image reconstruction. These include corrections for random coincidences, scatter, and dead time in the emission scan, as well as attenuation correction (usually performed by a transmission and blank scan). After normalization corrections of the detectors, the attenuated-corrected PET data is reconstructed to produce quantitative images. The units are either given in % injected dose per gram tissue (ID/g) or in standardized uptake values (SUVs). However, due to the limited spatial resolution of currently available preclinical PET scanners, partial volume effects are present (e.g. in regions of the brain in rodents) as the distance between emission and annihilation of the positron leads to an underestimated intensity, since the activity signal is distributed over a larger volume (*129*).

The ultimate achievable PET resolution is limited by the error due to the positron range and noncolinearity of the annihilation photons since positron and electron are not exactly at rest when they annihilate and cause annihilation photons to differ in their momentum, hence being emitted not exactly 180° apart (*130*).

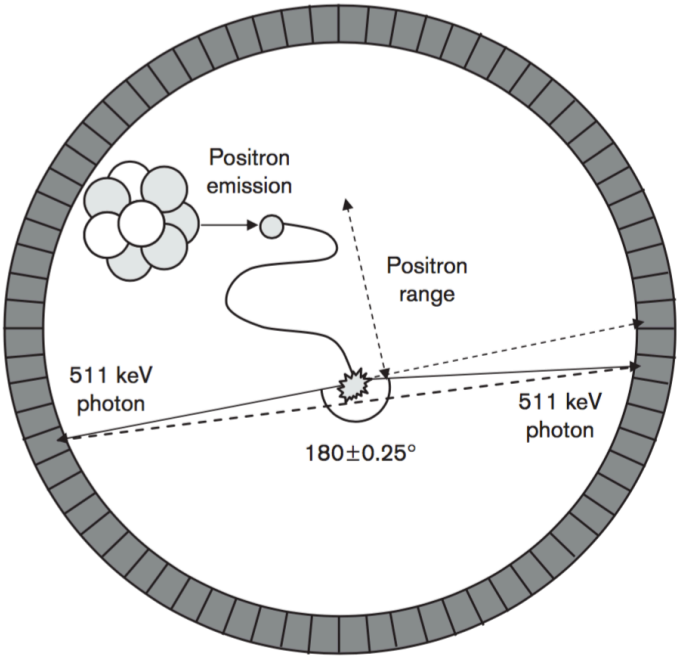

Figure 9: Schematic representation of the PET process. Two 511 keV photons result from the annihilation of the formed positronium of the decaying radioisotope. The γ irradiation is detected by two opposite detector units connected via a coincident circuit – © LWW Journals (122).

The positron range depends on both decay characteristics of the nuclide (e.g. ^{68}Ga 1.89 MeV, ^{18}F 633 keV (*131*)) and composition of surrounding media/tissue (*132*); an example of how the positron range affects image quality is given in Figure 10 (*129*). Typical preclinical PET scanners have spatial resolutions in the order of 1 – 2 mm while spatial resolution limitations of current clinical PET scanners are on the order of 4 mm (*133*). Because of current spatial resolution limitations in clinical PET scanners, the effect of lower-energy PET radionuclides such as ^{18}F or ^{11}C have indicated that improvements will not be significant for clinical scanners and will play a more noticeable role in small animal scanners (*133,134*).

Often, the change in the biodistribution of radiopharmaceuticals within the body offers the most important information about (patho)physiological processes. In order to get information about the kinetics of the injected radiotracer or its metabolites, dynamic PET scans are performed. Hereby, sequential series of PET images are collected as the tracer distributes in the body, hence giving the injected activity concentration as a function of time (*125*).

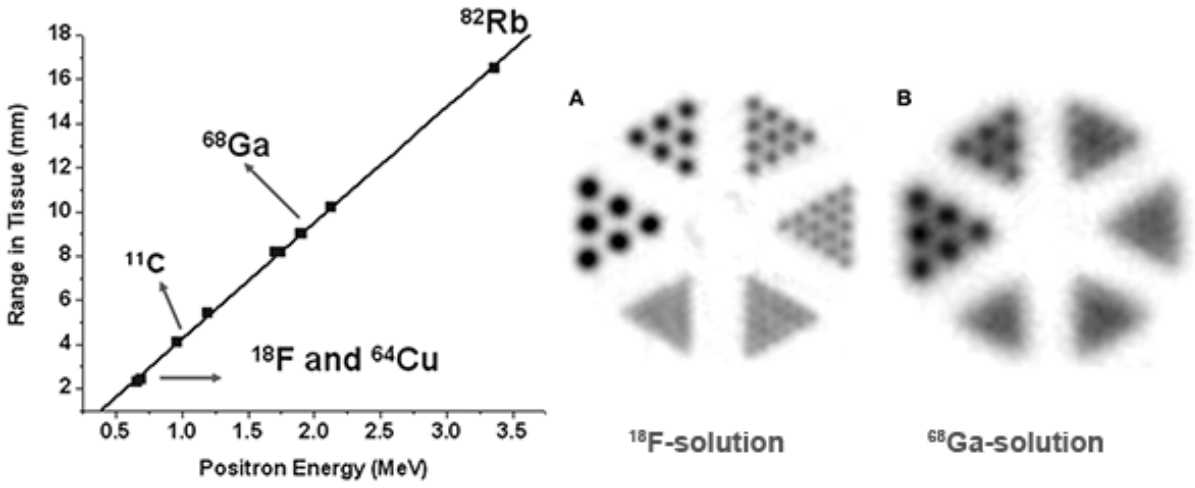

Figure 10: Positron range of different radionuclides as a function of their positron energy (119) and an example of how the positron range affects image quality (emission image of a mini-Derenzo phantom filled with A) ^{18}F-solution, B) ^{68}Ga solution) (129).

I.7 SPECT Tracers for Imaging of CXCR4

In chapter I.7 and I.8, a brief overview of developed SPECT and PET tracers for imaging of CXCR4 expression is given; for additional information, the reader is referred to excellent reviews on CXCR4 imaging probes (*18,84,86,87,135,136*).

[^{125}I]CPCR4 and [^{111}In]Ac-TZ14011 were the first reported imaging agents for CXCR4 expression. The cyclic pentapeptide [^{125}I]CPCR4 showed clear delineation of CXCR4^{+} tumors (5.5% ± 1.5% ID/g, 1h post injection (p.i.) *in vivo* and a rapid blood clearance accompanied by accumulation in the liver, intestines and kidney (*56*). The peptide Ac-TZ14011 was conjugated to DTPA via the side chain of D-Lys^{8} and subsequently radiolabeled with ^{111}In for SPECT imaging of CXCR4 (*40*). *In vivo* imaging showed rapid clearance of the peptide from the blood, however accumulation and retention of the tracer in liver, kidneys, and spleen while uptake in the tumor was very low (0.51% ID/g, 1h p.i.). [^{111}In]DTPA-TF14016, an analogue with an N-terminal 4-fluorobenzoyl group was subsequently reported offering higher CXCR4 affinity (*137*).

[^{111}In]AcTZ14011-MSAP was also used as multimodal imaging agent; however, conjugation of an additional fluorescent Cy5 derivative severely impaired the affinity towards CXCR4 (*78*). T/M ratios were similar to that of [^{111}In]Ac-TZ14011 with comparable high liver uptake. Dimeric and tetrameric derivatives with an improved affinity towards CXCR4 were also developed and T/M ratios were improved for the dimer due to decreased nonspecific muscle uptake (*79*). The tetramer displayed lower T/M ratios due to a decreased tumor uptake.

An ^{125}I-labeled anti-CXCR4 monoclonal antibody, [^{125}I]12G5, was used for SPECT imaging of CXCR4 expression in glioblastoma bearing U87-transfected mice (*138*). Although accumulation of the tracer in the tumor was given, its application is limited by high unspecific accumulation of labeled non-specific antibody in the tumors.

MAS3-CXCL12, the endogenous ligand of CXCR4 was labeled with ^{99m}Tc via a MAS3 chelator for imaging of CXCR4 expression after myocardial infarction (*139*). The tracer accumulated in heart tissue, however, the contribution of CXCR7 for ligand binding was not evaluated.

AMD3100 has been labeled with ^{99m}Tc and analyzed in tumor xenografts for SPECT imaging of CXCR4 expression (*60,63*). [^{99m}Tc]O2-AMD3100 showed three-fold reduced receptor affinity compared to [^{64}Cu]AMD3100 accompanied by negligible internalization. Although tumors were specifically delineated in a PC-3 prostate cancer model, uptake in the tumor and also the image contrast were lower as compared to its ^{64}Cu PET analog.

I.8 PET Tracers for Imaging of CXCR4

AMD3100 was labeled with ^{64}Cu and evaluated both in normal mice (*67*) showing rapid clearance from the blood and accumulation in CXCR4 expressing organs as well as in tumor-bearing mice (*64,66*). AMD3100, as well as [^{64}Cu]AMD3465 which showed very high accumulation in CXCR4^{+} tumors (*65*), the main drawback of both tracers is their high accumulation in the liver (>30-40 % ID/g, 1.5h p.i.) and kidneys.

Recently, the central bridging phenyl group in AMD3100 has been functionalized without a significant loss in CXCR4 affinity. New AMD3100 derivatives with prosthetic group for radiofluorination have been developed. A pinacol phenylboronate diester was designed as PET precursor, however, not yet radiolabeled and evaluated *in vivo* (*58*).

The peptide T140 has been used as a scaffold for the synthesis of CXCR4 imaging probes because of its high affinity for CXCR4. T140 was labeled with ^{18}F via an N-terminal fluorobenzoyl group and evaluated *in vivo* (*57*). [^{18}F]T140 had CXCR4-independent binding to red blood cells (RBCs) with the additional disadvantage of a long synthesis time with relatively low radiochemical yields (*57,86*). Injecting the tracer in low specific activity could overcome binding to RBCs, nevertheless, differences between non-CXCR4 and CXCR4^{+} tumors were statistically insignificant.

[^{64}Cu]/[^{68}Ga]T140-2D, T140 derivatives containing two DOTA chelators attached to the lysine residues Lys^{7} and D-Lys^{8} of T140, were labeled with ^{64}Cu or ^{68}Ga, respectively (*76*). Compared to [^{18}F]T140 the synthesis time was reduced, however binding to RBCs as well as kidney uptake and retention remained high, while liver uptake increased for both compounds, thought to be due to transchelation of the radiometals.

In [^{68}Ga]DOTA-4FBn-TN14003, a single DOTA is attached to D-Lys^{8}. Binding affinity to CXCR4 was not changed as in T140-2D (*77*). In the peptides T140-NFBs, the N-terminal fluorobenzoyl group of T140 was replaced by DOTA or NOTA and labeled with ^{64}Cu (*75*). Significantly reduced CXCR4 affinity of both compounds confirm the idea that large functional groups attached to the N-terminus are detrimental for the affinity to CXCR4. Both analogues showed no binding to RBCs and specific binding to CXCR4. However, both tracers showed high unspecific accumulation in the liver due to transchelation. Another NOTA analogue, [^{18}F]AlF-NOTA-T140, showed feasible aqueous ^{18}F radiofluorination, nevertheless, the problem of high liver and kidney uptake remained (*73*).

In NO2A-TN14003, a NOTA-NHS ester was used for coupling, rather than p-SCN-Bn-NOTA in NOTA-NFB (*140*). NO2A-TN14003 labeled with ^{68}Ga, designated as [^{68}Ga]NOTA-NFB, showed improved clearance with high and specific uptake in target tissue, giving high T/M

(9.5) and T/B ratios. Combined with a favorable dosimetry, the tracer was clinically analyzed in glioma patients (*141*).

In an effort to synthesize an ^{18}F-labeled T140 derivative with reduced binding to RBCs, Ac-TC14012 was labeled with two different ^{18}F prosthetic groups on Lys^{7} (*74*), respectively, as Lys^{7} is non-essential for binding to CXCR4 (*32*). [^{18}F]FB-Ac-TC14012 and [^{18}F]FP-Ac-TC14012, employing 4-fluorobenzoyl and 2-fluoropropionyl groups, respectively, showed overall decreased CXCR4 binding compared to Ac-TZ14012 and N-terminally 4-fluorobenzoyl labeled derivatives, accompanied with high uptake in the liver (~20% ID/g) and kidneys.

Moreover, monomeric and dimeric Ac-TZ14011 derivatives, DOTA-TZ1 and DOTA-TZ2 have been developed (*142*). Both peptides were used for ^{68}Ga labeling. The dimer showed both higher cellular uptake as well as 20-fold higher affinity to CXCR4 as compared to the monomer. [^{68}Ga]CPCR4.2-dimer showed limited tumor accumulation and high accumulation in the liver (~44% ID/g) (*81*).

The pentapeptide [^{68}Ga]pentixafor showed very efficient CXCR4 targeting exhibiting high accumulation in CXCR4^{+} tumors, a fast renal excretion and compared to other evaluated tracers, very low unspecific accumulation in the background. Within the presented thesis, three further analogues of pentixafor are presented as PET imaging agents for CXCR4 expression including an ^{18}F, ^{68}Ga, and ^{64}Cu derivative. For further information, the manuscripts are further explained in chapter III and the complete manuscripts can be found in the appendix.

The small molecule MSX-122 was labeled with ^{18}F and showed binding to CXCR4, however was not evaluated *in vivo* so far (2013).

I.9 Peptide Receptor Radionuclide Therapy

Including surgery and external radiation therapy, there is often no curative treatment available for a large group of patients with disseminated carcinomas. Radionuclide therapy represents an interesting (complementary) option to current treatment modalities because it permits the delivery of a high dose of therapeutic radiation to cancer cells while minimizing exposure of normal cells (*143*). Due to the fundamental linkage of the CXCR4/CXCL12 axis to cancer progression and metastasis, the CXCR4 receptor holds great potential for targeted radionuclide therapy. The specific activity of the peptide should be as high as possible to reach the maximal achievable absorbed dose in the tumor. Since radionuclide-conjugated peptides are administered in low mass amounts, unwanted side effects like the mobilization of stem cells in the case of CXCR4-targeting peptides are very unlikely to occur whereas ionizing irradiation is effectively delivered to the target. Before treatment, peptides can be radiolabeled with diagnostic radionuclides to identify receptor-positive tumor lesions, for treatment planning, and also dosimetry. Exchange to a therapeutic radionuclide, often by using the same peptide-conjugate, enables targeted radionuclide therapy. DOTATATE for instance has been labeled with different radionuclides for diagnosis (mainly ^{111}In and ^{68}Ga) and also treatment (mainly ^{177}Lu and ^{90}Y) of neuroendocrine tumors (*144-146*).

The decay properties of radionuclides, e.g. β^- or α emission, emission energy, linear energy transfer (LET), and half-life are important characteristics for diagnosis and therapy and can be chosen individually, depending on the type of the tumor, its size, intratumoral distribution (i.e. degree of heterogeneity of radionuclide deposition), pharmacokinetics, and other factors. ^{177}Lu for instance (β^-, E_{max} 0.5 MeV, tissue range$_{max}$ 2 mm (*144,147*) is more appropriate for smaller tumors, while ^{90}Y (β^-, E_{max} 2.3 MeV, tissue range$_{max}$ 12 mm (*144,147*), may be beneficial for larger lesions with heterogeneous receptor expression (*144,147,148*). Compared to β-particles (LET: 0.1-1 keV/µm) and γ irradiation, the local density of ionizations along a track of α-particles is considerably higher because multiple ionizations (60-230 keV/µm) occur in the immediate vicinity of the decay site (*149*). Hence, α-particle emitters can be beneficial to target single cancer cells, i.e. micro-metastases, which are difficult to treat by currently employed techniques (*150*). Moreover, the high specific ionization of α-emitters causes a higher fraction of double strand breaks and can break radio- and chemoresistance (*151*). Furthermore, cell death due to α-irradiation is minimally dependent on tumor oxygenation, which means that cells are killed effectively even in hypoxic areas of the tumor (*152,153*). Accordingly, the therapeutic potential of α-emitters like ^{211}At, ^{213}Bi, and ^{225}Ac have been investigated in some early stage clinical trials (*149,150,154*). An overview of selected radionuclides for therapy is given in Table 3.

On a large scale, only a few radionuclide therapies are routinely used. ^{131}I for instance is relatively inexpensive and can be used for imaging and therapy. In radioimmunotherapy, the β-particle emitting isotopes ^{131}I and ^{90}Y have been employed in >95% of clinical radioimmunotherapy trials (*155,156*). Proteins labeled with ^{131}I however, degrade quickly when endocytosed in tumor cells and result in the release of ^{131}I-tyrosine and free ^{131}I into the blood stream (*157*). In general the use of ^{131}I in PRRT has not been particularly successful. Bakker et al. for instance reported on the extensive radiolytic decomposition of octreotide for therapeutic doses of ^{131}I-labeled octreotide for therapy of neuroendocrine tumors (*158*). Clinical trials of ^{177}Lu and ^{67}Cu (*159-161*) as well as current and clinical prospects of therapeutic radionuclides in nuclear medicine can be found in the literature (*162-164*).

Regarding CXCR4, various CXCR4 antagonists have been developed and some are investigated as anticancer agents (*165*). The majority of these agents aim towards blocking the CXCR4 receptor, hence interfering in cell migration processes and positively affecting overall survival. Nevertheless, the effect on tumor growth by antagonizing CXCR4 alone has only a negligible effect and is more efficient with combined chemotherapy. Throughout the thesis, several new pentixafor-based imaging agents for CXCR4 were developed. Selected structural modifications of the pentixafor scaffold lead to pentixather (*cyclo*(-D-Tyr(3-I)-N-Me-D-Orn(AMB, DOTA)-L-Arg-L-2-Nal-Gly-)), which provides a molecular scaffold with higher flexibility towards structural modifications (*166,167*). Pentixather labeled with potential nuclides for endoradiotherapy (e.g. ^{90}Y, ^{177}Lu, ^{213}Bi) showed high receptor affinities (chapter III.6 and appendix) and [^{90}Y/^{177}Lu]pentixather already demonstrated promising results in patients with multiple myeloma (*167*).

Table 3: Physical decay properties of selected therapeutic radionuclides (*168*)

Isotope	Half-life	Decay	E_{max} [MeV]	Mean range [mm]
^{90}Y	2.7 d	β^-	2.3	2.76
^{131}I	8.0 d	β^-, γ	0.81	0.40
^{177}Lu	6.7 d	β^-, γ	0.50	0.28
^{186}Re	3.8 d	β^-, γ	1.1	0.92
^{188}Re	17 h	β^-, γ	2.1	2.43
^{67}Cu	2.6 d	β^-, γ	0.57	0.6
^{211}At	7.2 h	α	5.87	0.04-0.1
^{213}Bi	45.7 min	α	5.87	0.04-0.1
^{225}Ac	10 d	α, β^-	5.83	0.04-0.1

II. Objective

The objective of the presented thesis was the development of diagnostic and therapeutic radiopharmaceuticals targeting the chemokine receptor CXCR4. The overexpression of CXCR4 in at least 30 different types of cancers makes the receptor an attractive diagnostic and therapeutic target. Amongst several reported imaging agents for CXCR4, only one compound, [^{68}Ga]pentixafor, has completed initial evaluation in humans and no tracer for PRRT of CXCR4-positive cancer cells has been reported.

Targeting the CXCR4 receptor with small cyclic pentapeptides remains challenging, because minor structural modifications within the peptide or linker-chelate structure often significantly affect the receptor affinity. The study was therefore aimed at investigating different (radio)labeled peptides in terms of efficient CXCR4-targeting properties *in vitro* and *in vivo* with the final objective to open new perspectives towards individualized cancer diagnostics and therapies.

Based on the unique CXCR4 targeting properties of [^{68}Ga]pentixafor, the pentixafor scaffold was used to investigate various linker-chelate structures to broaden the spectrum of applicable (radio)metal-labeled pentixafor analogs for diagnostics (labeling with ^{68}Ga, ^{18}F, ^{64}Cu) and endoradiotherapeutic use (^{90}Y, ^{177}Lu). Moreover, the lack of an ^{18}F-labeled pentixafor-based tracer for PET imaging of CXCR4 expression *in vivo* necessitated the synthesis of an ^{18}F-labeled CXCR4-targeting peptide. Besides the development of an ^{18}F-based peptide for PET imaging of CXCR4 expression, the objective of the thesis was the synthesis of a Cu-labeled peptide as theranostic probe for both PET imaging (^{64}Cu) as well as potential endoradiotherapeutic agent (labeled with ^{67}Cu). Targeted radionuclide therapy gains increasing importance in personalized nuclear medicine and, unlike conventional external beam therapy, causes less damage to normal tissues; a further objective was therefore the development of peptides suitable for labeling with therapeutic radionuclides (e.g. ^{67}Cu, ^{177}Lu, ^{90}Y, ^{213}Bi) for PRRT.

III. Results – Publication Summaries and Bibliographic Data

This chapter primarily outlines the reported project and logical order of the development of diagnostic and therapeutic radiopharmaceuticals that target the chemokine receptor 4. Rather than the scientific details available in the attached original peer-reviewed publications (Appendix 1-8), the overall idea and achieved success should be apparent to the reader in brief. Moreover, the bibliographic data of each publication is listed including a link to the formal publication as well as the relevant DOI.

III.1 The influence of different metal-chelate conjugates of pentixafor on the CXCR4 affinity

Andreas Poschenrieder[1]*, Margret Schottelius[1], Markus Schwaiger[2], Horst Kessler[3], and Hans-Jürgen Wester[1]

[1] Pharmaceutical Radiochemistry, Technical University Munich, Walther-Meißner-Str.3, 85748 Garching, Germany

[2] Department of Nuclear Medicine, Technical University Munich, Klinikum rechts der Isar, Ismaninger Straße 22, 81675 München, Germany

[3] Institute for Advanced Study at the Department Chemie, Technical University Munich, Lichtenbergstr. 2a, 85748 Garching, Germany

*To whom correspondence should be addressed

Originally published in: EJNMMI Research
DOI: 10.1186/s13550-016-0193-8
Hyperlink: http://ejnmmires.springeropen.com/articles/10.1186/s13550-016-0193-8

This study deals with the synthesis of pentixafor-based peptides consisting of the sequence (*cyclo*(-D-Tyr-N-Me-D-Orn(linker-chelate)-L-Arg-L-2-Nal-Gly-) and the evaluation of their affinity towards CXCR4. Major objective of the present study was to broaden the spectrum of applicable radio(metal)-labeled pentixafor analogs for diagnostic or therapeutic purposes.

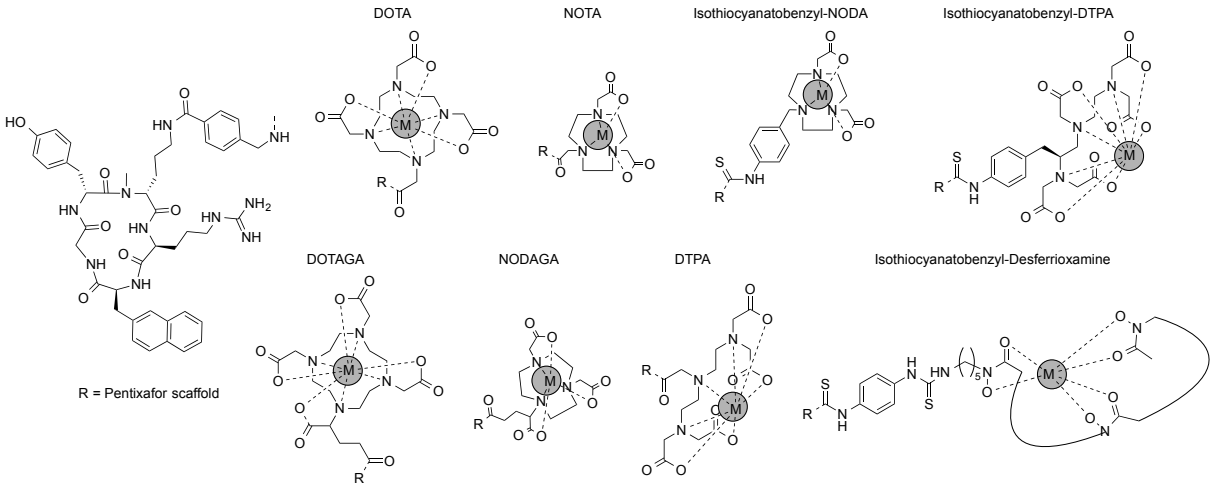

Figure 11: Structures of synthesized pentixafor-based analogs with different chelators and metals (M, gray) relevant for medical applications.

For this purpose, seven different chelators have been coupled to the D-Orn side chain of the pentapeptide core with or without AMB as the linker, (a) DOTA, (b) 1,4,7,10-tetraazacyclododecane,1-(glutaric acid)-4,7,10-triacetic acid (DOTAGA), (c) NOTA, (d) 1,4,7-triazacyclononane,1-glutaric acid-4,7-acetic acid (NODAGA), (e) DTPA, (f) 2-(4-isothiocyanatobenzyl) (p-SCN-Bn)-DTPA, (g) p-SCN-Bn-DFO, and (h) 2,2'-(7-(4-isothiocyanatobenzyl)-1,4,7-triazonane-1,4-diyl)diacetic acid (NCS-MP-NODA) (Figure 11). Depending on the chelator, the peptide conjugates were labeled with Ga^{3+}, AlF^{2+}, Zr^{4+}, Cu^{2+}, In^{3+}, Y^{3+}, Lu^{3+}, and Bi^{3+} relevant for medical applications.
The binding affinity of pentixafor derivatives towards CXCR4 was greatly influenced by chelator and metal exchange. For example, affinities varied between 17.6 nM to 1165 nM for Ga-NOTA and Cu-DOTAGA conjugated to the same highly affine pentixafor scaffold. Furthermore, it was confirmed that Ga-pentixafor represents a highly optimized ligand.

Within 30 metal-free or metal-labeled synthesized analogs, two new conjugates with an improved affinity compared to the parental compound [^{68}Ga]pentixafor have been identified, namely [^{nat}Ga]NOTA-pentixafor and [^{nat}Bi]DOTA-pentixafor. While the Ga^{3+} cation is known to form kinetically and thermodynamically more stable complexes with NOTA compared to the larger DOTA macrocycle, the Bi^{3+}-complex is expected to be a very promising new ligand for further studies towards α-emitter-based endoradiotherapeutic approaches.

III.2 Preclinical evaluation of [^{68}Ga]NOTA-pentixafor for PET imaging of CXCR4 expression *in vivo* - a comparison to [^{68}Ga]pentixafor

Andreas Poschenrieder[1]*, Margret Schottelius[1], Markus Schwaiger[2], and Hans-Jürgen Wester[1]

[1] Pharmaceutical Radiochemistry, Technische Universität München, Walther-Meißner-Str.3, 85748 Garching

[2] Nuklearmedizinische Klinik und Poliklinik, Klinikum rechts der Isar, Technische Universität München, Ismaningerstr. 22, 81675 München

*To whom correspondence should be addressed

Originally published in: EJNMMI Research
DOI: 10.1186/s13550-016-0227-2
Hyperlink: http://ejnmmires.springeropen.com/articles/10.1186/s13550-016-0227-2

In the presented work [^{68}Ga]NOTA-pentixafor was evaluated as a PET imaging agent for CXCR4 expression *in vivo* and compared to [^{68}Ga]pentixafor. [^{nat}Ga]NOTA-pentixafor showed the highest affinity towards CXCR4 amongst various radio(metal)-labeled pentixafor analogs, including [^{nat}Ga]pentixafor, in a previous study (*169*). Moreover, NOTA is well known to form kinetically and thermodynamically stable complexes with Ga^{3+}, with superior stability than Ga-DOTA (*170*).

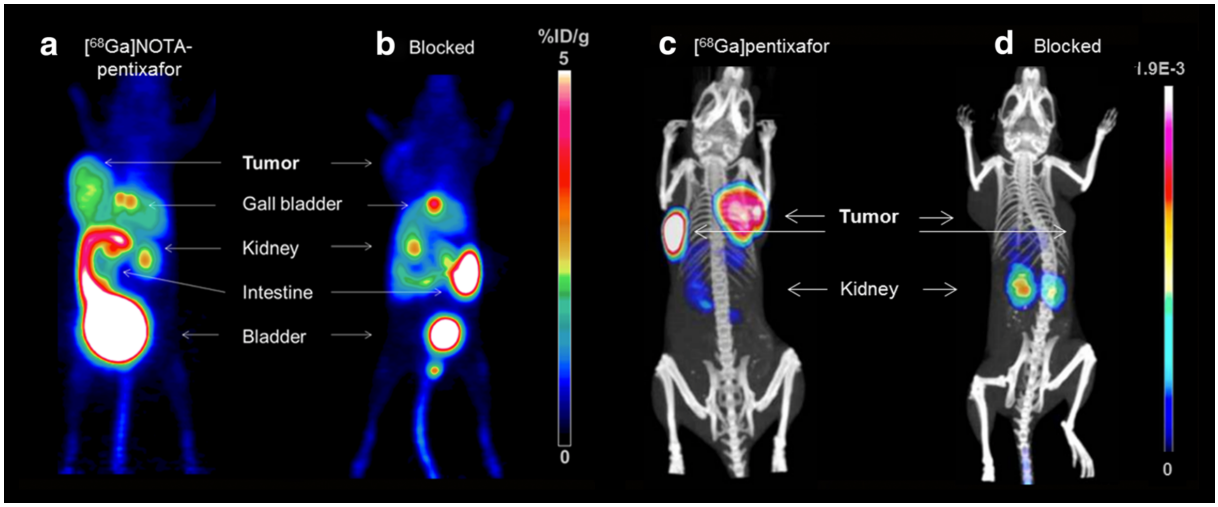

Figure 12: μPET/(CT) images of tumor bearing mice at 1.5h p.i. – a comparison of [^{68}Ga]NOTA-pentixafor (a) to [^{68}Ga]pentixafor (c). (b) and (d): co-injection of 2 mg/kg AMD3100. Credit c and d: © 2015 Ivyspring Int. Publisher.

As a consequence, [^{68}Ga]NOTA-pentixafor was preclinically evaluated as potential PET imaging agent. It has been shown that, despite improved CXCR4 affinity, the CXCR4 targeting efficiency of [^{68}Ga]NOTA-pentixafor was substantially compromised compared to [^{68}Ga]pentixafor. The GaNOTA-for-GaDOTA exchange alters the overall charge of the chelator moiety, also leading to a change in lipophilicity of [^{68}Ga]NOTA-pentixafor (logP = -2.4) compared to the DOTA analog (logP = -2.9). Moreover, the internalization efficiency into CXCR4-positive Chem-1 cells was substantially decreased for the Ga-NOTA conjugate. Accordingly, PET images and biodistribution studies of Daudi xenografts revealed significantly lower uptake of [^{68}Ga]NOTA-pentixafor in the tumor and higher unspecific accumulation in non-target tissue compared to [^{68}Ga]pentixafor (Figure 12). Although [^{68}Ga]NOTA-pentixafor showed low tumor-to-organ ratios, CXCR4 uptake was specific as demonstrated by co-injection of AMD3100, and tumors were clearly delineated in small-animal PET images.

The study demonstrated the strong influence of the chelator on the pharmacokinetics of pentixafor-based tracers. It has been shown that [^{68}Ga]NOTA-pentixafor offers no advantages over [^{68}Ga]pentixafor. In addition, it outlines the excellent CXCR4 targeting characteristics of [^{68}Ga]pentixafor for successful imaging of CXCR4 expression.

III.3 An optimized strategy for the mild and efficient solution phase iodination of tyrosine residues in bioactive peptides

Margret Schottelius[1,*], Matthias Konrad[1], Andreas Poschenrieder[1], Theresa Osl[1], and Hans-Jürgen Wester[1]

[1] Chair for Pharmaceutical Radiochemistry, Technical University Munich, Walther-Meissner-Strasse 3, 85748 Garching, Germany

[*]To whom correspondence should be addressed

Originally published in: Tetrahedron Letters
DOI: 10.1016/j.tetlet.2015.10.032
Hyperlink: http://dx.doi.org/10.1016/j.tetlet.2015.10.032

The publication presents an efficient way for the direct (mono)iodination of unprotected tyrosine-containing peptides. Usually, 3-iodo-Tyr is introduced into the peptide sequence by time-consuming de novo solid phase peptide synthesis. Concerning the direct tyrosine iodination from unprotected precursor peptide, there is only one procedure described in literature using chloramine-T, which was used for very low amounts of somatostatin-targeting peptides (< 70 nmol) (*171*). The study therefore aimed to provide a mild and efficient solution phase iodination of tyrosine residues in peptides for the small to medium-scale (~ 20 mg).

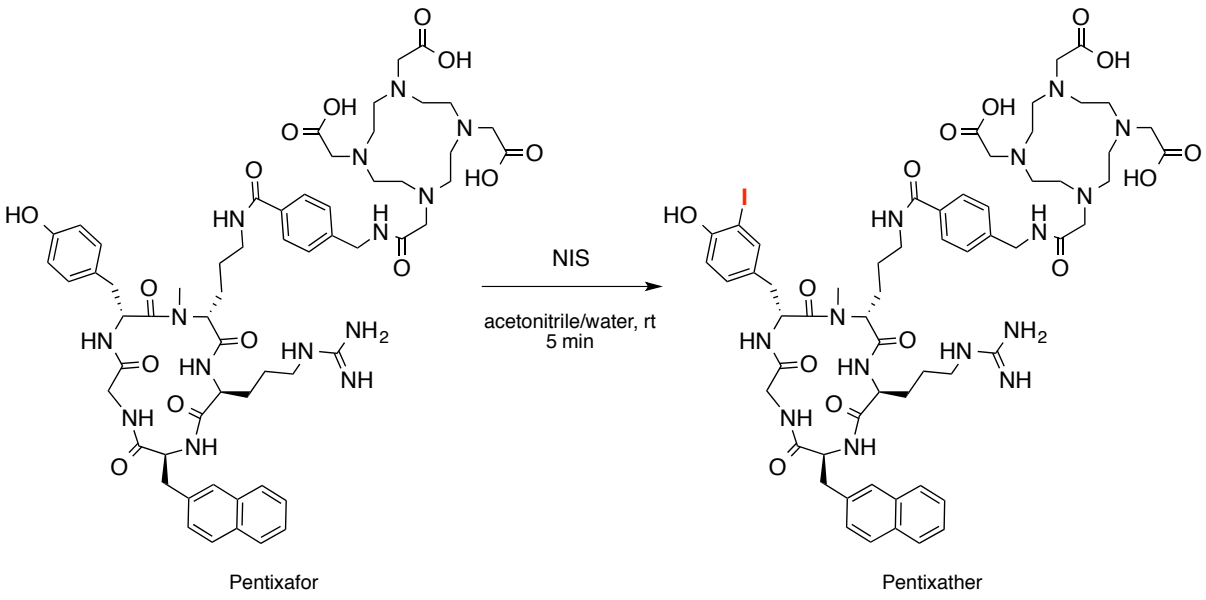

Figure 13: Direct iodination of unprotected tyrosine-containing pentixafor using N-iodosuccinimide.

In the manuscript, different methods for the direct tyrosine iodination are described. It was shown that the use of *N*-iodosuccinimide (NIS) in a 1:1 mixture of acetonitrile/water (v/v) resulted in the highest turnover rates into iodinated species and the fastest procedure (5 min, rt) with broad applicability for many peptides. Using 0.35 equiv. of NIS led to the highest yields for pentixather up to 48%, whereas higher molar ratios of NIS resulted in higher amounts of unwanted di-iodinated compound (Figure 13). Acetonitrile/water was used as the solvent because of the excellent solubility of various peptides in this system.

The reported method enables the fast, mild, and efficient iodination of Tyr-residues in bioactive compounds on a small (<1 mg) to medium scale (1-20 mg). Moreover, fine-tuning of the molar ratio of NIS allows for easy control over product-to-side product ratios with the possibility to recover unreacted starting peptide during preparative HPLC.

III.4 First ^{18}F-labeled pentixafor-based imaging agent for PET imaging of CXCR4-expression *in vivo*

Andreas Poschenrieder,[1,*] Theresa Osl,[1] Margret Schottelius,[1] Frauke Hoffmann,[1] Martina Wirtz,[1] Markus Schwaiger,[2] and Hans-Jürgen Wester[1]

[1] Pharmaceutical Radiochemistry, Technische Universität München, Walther-Meißner-Str.3, 85748, Garching, Germany

[2] Nuklearmedizinische Klinik und Poliklinik, Technische Universität München, Ismaningerstr. 22, 81675 München, Germany

[*]To whom correspondence should be addressed

Originally published in: Tomography
DOI: 10.18383/j.tom.2016.00130
Hyperlink: http://digitalpub.tomography.org/i/698373-vol-2-no-2-jun-2016/12

The idea of study was the synthesis of an ^{18}F-labeled imaging agent based on pentixafor in order to combine the excellent CXCR4-targeting properties of [^{68}Ga]pentixafor with the favorable radionuclide properties of ^{18}F.

Within numerous imaging agents targeting CXCR4, e.g. T140 and AMD3100 derivatives, [^{68}Ga]pentixafor holds a unique position regarding CXCR4 targeting efficiency and pharmacokinetics.

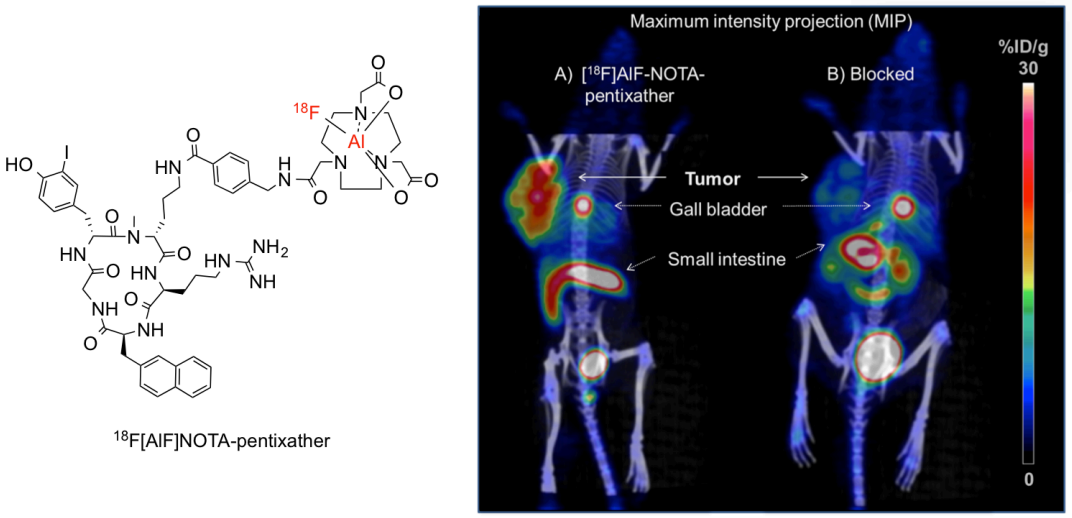

Figure 14: Structure of [^{18}F]AlF-NOTA-pentixather and PET/CT images of Daudi xenograft bearing mice at 1h p.i.; (a) tracer only, (b) coinjection of 50 µg AMD3100 (2mg/kg).

Since the radionuclide properties of ^{18}F are superior to those of ^{68}Ga in terms of positron energy and achievable spatial resolution in PET imaging, we synthesized a slightly modified pentixafor backbone suitable for conjugation with NOTA for straightforward aqueous radiofluorination. Using the radiolabeling approach of McBride et al. (*172*), radiochemical yields of 45.6% ± 13.3% were achieved with radiochemical purities of 98.0% ± 1.7%.

[^{18}F]AlF-NOTA-pentixather (Figure 14) showed both higher affinity towards CXCR4 as well as an increased internalization efficiency. Due to the increased lipophilicity of [^{18}F]AlF-NOTA-pentixather however, caused by the NOTA-for-DOTA exchange and the tyrosine iodination, a shift towards hepatobiliar excretion compared to [^{68}Ga]pentixafor was observed. Nevertheless, accumulation of [^{18}F]AlF-NOTA-pentixather in the Daudi tumor was higher than in all other organs and the tumor has been clearly delineated.

It was shown that for the first time, a pentixather derivative could be labeled with ^{18}F for high contrast PET imaging of CXCR4 expression *in vivo*.

III.5 [^{64}Cu]NOTA-pentixather enables high resolution PET imaging of CXCR4 expression in a preclinical lymphoma model

Andreas Poschenrieder[1], Margret Schottelius[1,*], Theresa Osl[1], Markus Schwaiger[2], and Hans-Jürgen Wester[1]

[1] Pharmaceutical Radiochemistry, Technische Universität München, Walther-Meißner-Str.3, 85748 Garching

[2] Department of Nuclear Medicine, Klinikum rechts der Isar, Technische Universität München, Ismaningerstr. 22, 81675 München

[*]To whom correspondence should be addressed

Originally published in: EJNMMI Radiopharmacy and Chemistry
DOI: 10.1186/s41181-016-0020-6
Hyperlink: https://ejnmmipharmchem.springeropen.com/articles/10.1186/s41181-016-0020-6

The publications presents the preclinical evaluation of [^{64}Cu]NOTA-pentixather as a high contrast PET imaging agent for CXCR4 expression *in vivo* (Figure 15). ^{64}Cu radionuclides represent an interesting imaging option since their comparably long half-life and low positron energy, comparably to that of ^{18}F, allow for kinetic PET imaging studies over extended

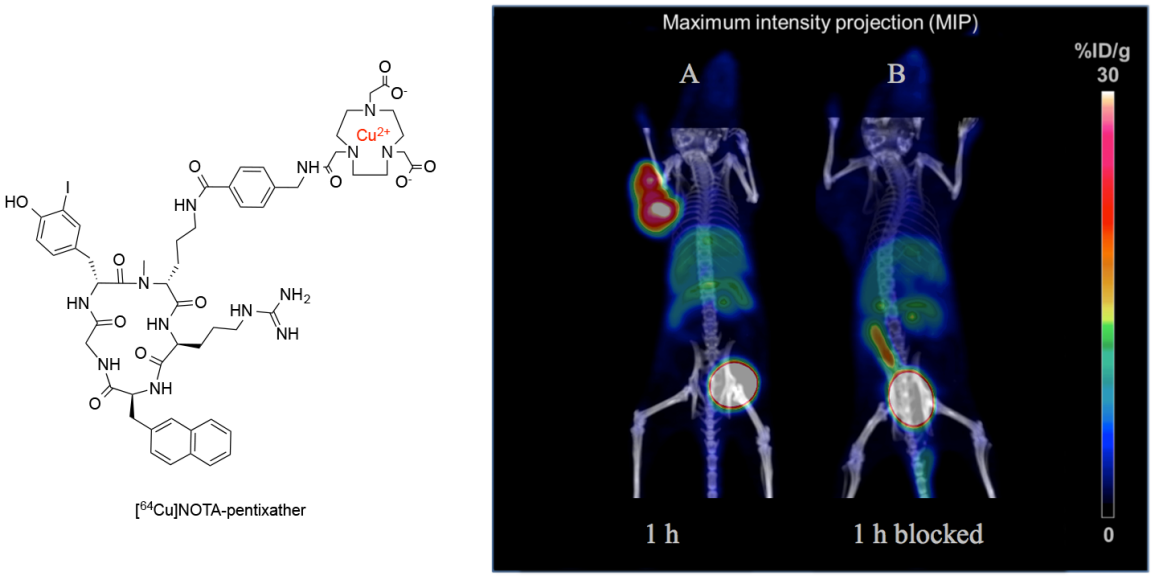

Figure 15: Structure of ^{64}Cu-1,4,7-triazacyclononane-triacetic acid (NOTA)-pentixather and according PET/CT images of Daudi xenograft bearing mice at 1h post injection (p.i.); (a) tracer only, (b) coinjection of 50 µg AMD3100 (2 mg/kg).

periods of time with high spatial resolution. Moreover, the possible exchange to the therapeutic radionuclide ^{67}Cu provides access to potential endoradiotherapeutic applications.

NOTA-pentixather was rapidly radiolabeled with ^{64}Cu with high radiochemical yields ≥90% and purities >99%. The stability of the complex was thoroughly tested by serum incubation and transchelation studies in EDTA using different pHs *in vitro* and also by metabolite studies *in vivo*. [^{64}Cu]NOTA-pentixather showed no metabolite formation in blood and urine within 1h p.i. and also demonstrated high resistance towards transchelation to serum proteins or EDTA. The tracer showed efficient CXCR4-targeting of the Daudi tumor *in vivo* (13.1% ± 1.5% ID/g) and tumor uptake was specific as shown by co-injection of AMD3100, which reduced CXCR4 uptake in the xenograft by 88%. While kidney uptake was comparably low (3.8% ± 0.5% ID/g), due to the enhanced lipophilicity (logP = -1.2) compared to [^{68}Ga]pentixafor (logP = -2.9), [^{64}Cu]NOTA-pentixather showed some uptake in excretory organs such as liver and intestines (7.2% ± 1.1% and 5.0% ± 2.8% ID/g, respectively).

It has been shown that the concept of pentixafor/pentixather-based CXCR4-targeted theranostics was successfully extended by a promising ^{64}Cu-labeled analog. While the tracer's efficiency for therapeutic use is limited by fast externalization kinetics and some uptake in the excretory organs, [^{64}Cu]NOTA-pentixather proved to be a promising imaging agent for CXCR4-PET imaging.

III.6 [^{177}Lu]pentixather: comprehensive preclinical evaluation of a first CXCR4-directed endoradiotherapeutic agent

Margret Schottelius[1,*], Theresa Osl[1], Andreas Poschenrieder[1], Frauke Hoffmann[1], Seval Beykan[4], Heribert Hänscheid[4], Katharina Franke[2], Markus Schwaiger[3], Ulrich Keller[2], Michael Lassmann[4], and Hans-Jürgen Wester[1]

1 Chair for Pharmaceutical Radiochemistry, Technische Universität München, Walther-Meissner-Strasse 3, 85748 Garching, Germany

2 III. Medical Department, Klinikum rechts der Isar, Technische Universität München, Ismaningerstr. 22, 81675 Munich, Germany

3 Department of Nuclear Medicine, Klinikum rechts der Isar, Technische Universität München, Ismaningerstr. 22, 81675 Munich, Germany

4 Department of Nuclear Medicine, University of Würzburg, Oberdürrbacher Str. 6, 97080 Würzburg, Germany

* to whom correspondence should be addressed

Originally published in: Theranostics
DOI: 10.7150/thno.19119
Hyperlink: http://www.thno.org/v07p2350.htm

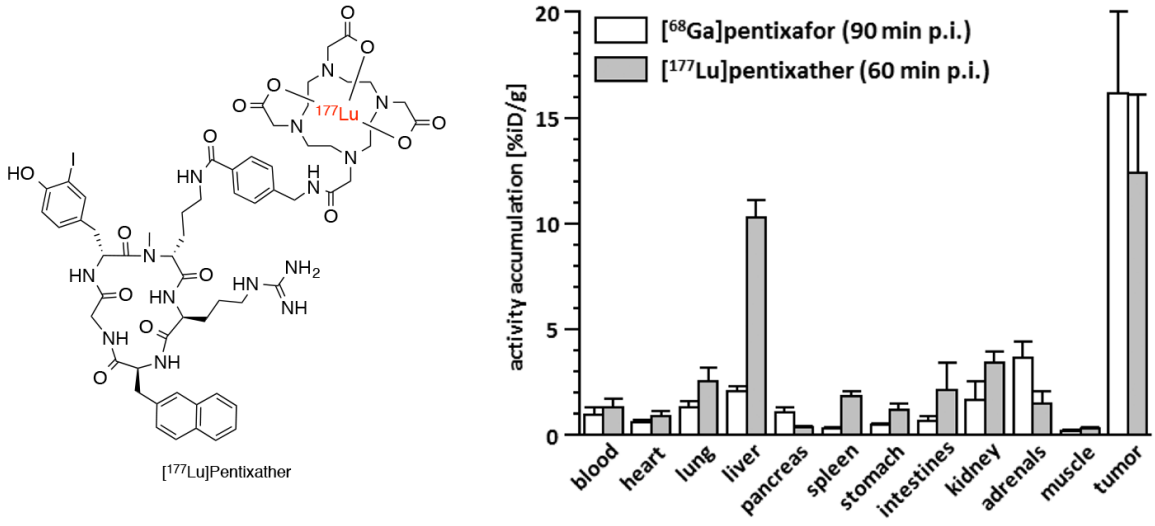

Figure 16: Structure of [^{177}Lu]pentixather and comparative biodistribution data of [^{68}Ga]pentixafor and [^{177}Lu]pentixafor in Daudi xenograft bearing mice (groups of n=5) at 1.5h and 1h p.i., respectively. Uptake values are given in % ID/g and are means ± SD.

The publication presents *[^{177}Lu]pentixather* as the first CXCR4-directed agent for peptide receptor radiotherapy. The efficiency of conventional chemotherapy of hematopoietic cancers and lympoproliferative diseases can be compromised by the recurrence of CXCR4-positive cells from protective niches that resisted chemotherapy. The interaction between CXCR4 and CXCL12 plays a significant role in the trafficking of CXCR4-expressing cells; moreover, CXCR4 is essential for metastatic spread to locations where CXCL12 is expressed and therefore allows tumor cells to access protective niches. Following the objective to directly target CXCR4-positive cancer cells and also their protective niche by cross-fire effect, we evaluated [^{177}Lu]pentixather preclinically for potential PRRT.

It was shown that [^{177}Lu]pentixather is stable *in vitro* and *in vivo* and demonstrates efficient CXCR4-targeting, characterized by high CXCR4 receptor affinity and high specific binding and selectivity to hCXCR4 with virtually no binding to mCXCR7 and only low specific binding to mCXCR4 and hCXCR7. Cellular binding of [^{177}Lu]pentixather correlated well with CXCR4 expression levels of various cell lines. Figure 16 shows the structure of [^{177}Lu]pentixather and its biodistribution in comparison to [^{68}Ga]pentixafor. Compared to the reference [^{68}Ga]pentixafor, [^{177}Lu]pentixather shows high initial uptake in all excretory organs, with a rapid clearance from stomach, intestines, and kidneys. Accumulation in the liver remained high, up to 7d p.i., however, was partially blocked by AMD3100, indicating also partial CXCR4-specificity. Accumulation of [^{177}Lu]pentixather in the tumor was high and persistent up to 7d p.i., supported by high plasma protein binding (>96%) and a lipophilicity of logP = -1.76 which delayed whole-body clearance.

The study demonstrates excellent CXCR4 targeting characteristics of [^{177}Lu]pentixather *in vitro* and *in vivo* combined with a suitable pharmacokinetic profile. [^{177}Lu]pentixather showed high tumor accumulation and retention as well as an overall favorable dosimetry, enabling high radiation doses during PRRT. Combined with [^{68}Ga]pentixafor as imaging agent, [^{177}Lu]pentixather shows high potential for the clinical endoradiotherapy of CXCR4-overexpressing malignancies, following a CXCR4-targeted theranostic concept towards individualized cancer therapies.

III.7 First-in-Human Experience of CXCR4-Directed Endoradiotherapy with ^{177}Lu- and ^{90}Y-Labeled Pentixather in Advanced-Stage Multiple Myeloma with Extensive Intra- and Extramedullary Disease

Ken Herrmann[1,2,3,#,*], Margret Schottelius[4,#], Constantin Lapa[1], Theresa Osl[4], Andreas Poschenrieder[4], Heribert Hänscheid[1], Katharina Lückerath[1], Martin Schreder[5], Christina Bluemel[1], Markus Knott[5], Ulrich Keller[6], Andreas Schirbel[1], Samuel Samnick[1], Michael Lassmann[1], Saskia Kropf[7], Andreas K. Buck[1], Hermann Einsele[5], Hans-Jürgen Wester[4‡], and Stefan Knop[5‡]

[1] Department of Nuclear Medicine, University Hospital Würzburg, Würzburg, Germany
[2] Department of Molecular and Medical Pharmacology, David Geffen School of Medicine at UCLA, Los Angeles, USA
[3] Jonsson Comprehensive Cancer Center, David Geffen School of Medicine at UCLA, Los Angeles, USA
[4] Pharmaceutical Radiochemistry, Technische Universität München, Munich, Germany
[5] Department of Internal Medicine II, Division of Hematology and Medical Oncology, Universitätsklinikum Würzburg, Würzburg, Germany
[6] III. Medical Department of Hematology and Medical Oncology, Technische Universität München, Munich, Germany
[7] Scintomics GmbH, Fürstenfeldbruck, Germany

[*]To whom correspondence should be addressed
[#]Ken Herrmann and Margret Schottelius contributed equally to this work
[‡]Hans-Juergen Wester and Stefan Knop contributed equally to this work

Originally published in: Journal of Nuclear Medicine
DOI: 10.2967/jnumed.115.167361
Hyperlink: http://jnm.snmjournals.org/content/57/2/248.long

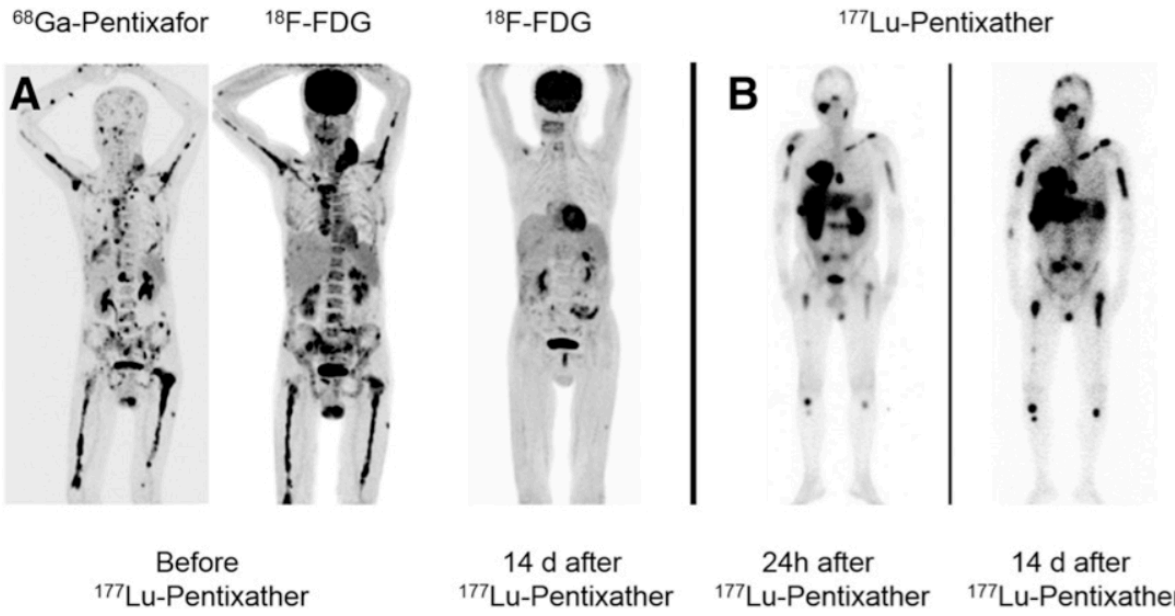

Figure 17: A) maximum intensity projections (MIPs) of [^{68}Ga]pentixafor and [^{18}F]FDG PET/CT indicate high CXCR4 expression in a patient with MM before pentixather therapy. The patient shows promising metabolic response 14 d after [^{90}Y]pentixather therapy, followed by external radiation therapy and subsequent autologous stem cell transplantation. B) Scintigraphic images confirm binding and retention of ^{177}Lu to the CXCR4 target.

The publication shows the first-in-human experience of pentixather, radiolabeled with ^{177}Lu or ^{90}Y, for CXCR4-targeted peptide receptor radiotherapy. Radiolabeled pentixather is an innovative therapeutic peptide for the specific targeting of CXCR4-positive cancer cells. The efficiency of systemic treatments like classical chemotherapy is often compromised because of homing of CXCR4 expressing cancer cells into protective microenvironments like the marrow, where adhesion to stromal elements may protect cancer cells from cytotoxic drugs (*22*). In the manuscript, the feasibility and high potential of [^{177}Lu/^{90}Y]pentixather endoradiotherapy is shown in patients with extensive intramedullary and extramedullary manifestations of multiple myeloma.

A remarkable therapeutic effect could be achieved in a MM patient that responded with a significantly reduced [^{18}F]FDG uptake after [^{177}Lu]- and [^{90}Y]pentixather therapy (Figure 17). It has been shown that CXCR4-directed endoradiotherapy with pentixather, combined with cytotoxic chemotherapy and autologous stem cell transplantation, is a potential novel treatment option especially for patients with advanced MM.

III.8 Imaging the cytokine receptor CXCR4 in atherosclerotic plaques with the radiotracer [^{68}Ga]pentixafor for positron emission tomography

Fabien Hyafil[1-2,*], Jaroslav Pelisek[3], Iina Laitinen[1], Margret Schottelius[4], Miriam Mohring[1], Yvonne Döring[5], Emiel P.C. von der Vorst[5], Michael Kallmayer[3], Katja Steiger[7], Andreas Poschenrieder[4], Johannes Notni[4], Johannes Fischer[8], Christine Baumgartner[8], Christoph Rischpler[1], Stephan Nekolla[1], Christian Weber[5], Hans-Henning Eckstein[3], Hans-Jürgen Wester[4], and Markus Schwaiger[1]

1 Department of Nuclear Medicine, Klinikum Rechts der Isar, Munich, Germany
2 Department of Nuclear Medicine, Bichat University Hospital, Paris, France
3 Department of Vascular and Endovascular Surgery, Klinikum Rechts der Isar, Munich, Germany
4 Pharmaceutical Radiochemistry, Technische Universität München, Garching, Germany
5 Institute for Cardiovascular Prevention, Ludwig-Maximilians-Universität München, Munich, Germany
6 Cardiovascular Research Institute Maastricht (CARIM), Maastricht University, Maastricht, The Netherlands
7 Department of Pathology, Klinikum Rechts der Isar, Munich, Germany
8 Centre of Preclinical Research, Klinikum Rechts der Isar, Munich, Germany

*To whom correspondence should be addressed

Originally published in: Journal of Nuclear Medicine
DOI: 10.2967/jnumed.116.179663
Hyperlink: http://jnm.snmjournals.org/content/58/3/499

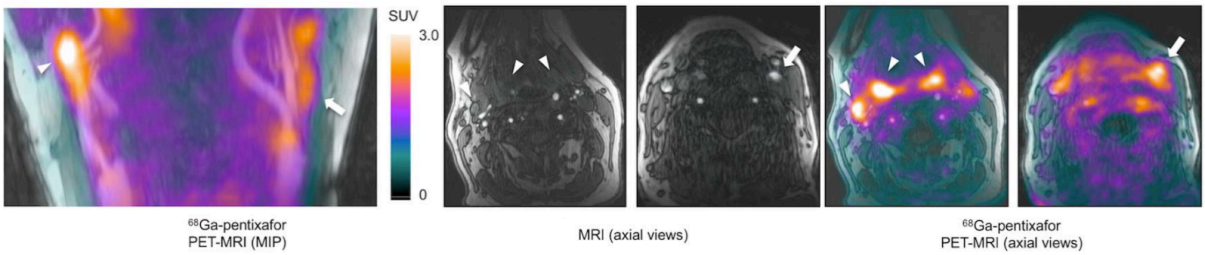

Figure 18: In vivo imaging of CXCR4 expression in human carotid atherosclerotic plaques with [^{68}Ga]pentixafor-PET/MRI. White arrows indicate carotid plaques with high [^{68}Ga]pentixafor uptake. White arrowheads indicate [^{68}Ga]pentixafor accumulation in lymph node and tonsils.

In this publication, [^{68}Ga]pentixafor was evaluated as potential PET imaging agent for CXCR4 expression in atherosclerotic plaques (Figure 18). Since CXCR4 is expressed on inflammatory cells, ^{68}Ga-labeled pentixafor was evaluated as a potential alternative to FDG to assess macrophage infiltration in atherosclerotic plaques in an experimental rabbit model.

[^{18}F]FDG PET is used to detect inflammation in cardiovascular imaging. However, FDG comes with a set of important limitations such as higher background signals of the blood, physiological uptake in the heart, and the need for fasting before imaging. [^{68}Ga]pentixafor was therefore investigated as alternative PET imaging agent to specifically target inflammatory cells in the vessel wall.

It has been demonstrated that [^{68}Ga]pentixafor shows high activity accumulation in atherosclerotic plaques of the abdominal aorta and right carotid artery as compared to the normal control arteries. Moreover, uptake of [^{125}I]pentixafor was partial specific as shown by pre-injection of AMD3100, which resulted in a ~40% reduced uptake. It could also be demonstrated that [^{125}I]pentixafor uptake in the vessel wall was located in macrophage-rich regions of atherosclerotic plaques and correlated with the intensity of CXCR4 expression.

The studies support the potential role of [^{68}Ga]pentixafor as a more specific PET imaging agent in comparison to FDG for the detection of CXCR4 expression in macrophage-infiltrating atherosclerotic plaques.

IV. Reprint Permissions

All manuscripts were reproduced by permission of the corresponding journals. The detailed bibliographic data and corresponding hyperlinks of the respective articles can be found in chapter III. Original publications can be found in the appendix.

IV.1 Springer Open Publications

Poschenrieder A, Schottelius M, Osl T, Schwaiger M, Wester H-J. [^{64}Cu]NOTA-pentixather enables high resolution PET imaging of CXCR4 expression in a preclinical lymphoma model. EJNMMI Radiopharmacy and Chemistry. 2017;2:2.

Poschenrieder A, Schottelius M, Schwaiger M, Wester H-J. Preclinical evaluation of [^{68}Ga]NOTA-pentixafor for PET imaging of CXCR4 expression in vivo - a comparison to [^{68}Ga]pentixafor. EJNMMIR. 2016;6(1):1-5.

Poschenrieder A, Schottelius M, Schwaiger M, Kessler H, Wester H-J. The influence of different metal-chelate conjugates of pentixafor on the CXCR4 affinity. EJNMMI research. 2016;6(1):1-8.

License agreement

In submitting an article to any of the journals published by SpringerOpen I certify that:

- I am authorized by my co-authors to enter into these arrangements.
- I warrant, on behalf of myself and my co-authors, that:
    - the article is original, has not been formally published in any other peer-reviewed journal, is not under consideration by any other journal and does not infringe any existing copyright or any other third party rights;
    - I am/we are the sole author(s) of the article and have full authority to enter into this agreement and in granting rights to Springer are not in breach of any other obligation;
    - the article contains nothing that is unlawful, libellous, or which would, if published, constitute a breach of contract or of confidence or of commitment given to secrecy;
    - I/we have taken due care to ensure the integrity of the article. To my/our - and currently accepted scientific - knowledge all statements contained in it purporting to be facts are true and any formula or instruction contained in the article will not, if followed accurately, cause any injury, illness or damage to the user.

- I, and all co-authors, agree that the article, if editorially accepted for publication, shall be licensed under the Creative Commons Attribution License 4.0. If the law requires that the article be published in the public domain, I/we will notify Springer at the time of submission, and in such cases the article shall be released under the Creative Commons 1.0 Public Domain Dedication waiver. For the avoidance of doubt it is stated that sections 1 and 2 of this license agreement shall apply and prevail regardless of whether the article is published under Creative Commons Attribution License 4.0 or the Creative Commons 1.0 Public Domain Dedication waiver.
- I, and all co-authors, agree that, if the article is editorially accepted for publication in *Chemistry Central Journal, Chemical and Biological Technologies in Agriculture, Geochemical Transactions, Heritage Science, Journal of Cheminformatics,* or *Sustainable Chemical Processes,* data included in the article shall be made available under the Creative Commons 1.0 Public Domain Dedication waiver, unless otherwise stated. For the avoidance of doubt it is stated that sections 1, 2, and 3 of this license agreement shall apply and prevail.

[End of SpringerOpen's license agreement]

IV.2 Tomography Publications

Poschenrieder A, Osl, T, Schottelius, M, Hoffmann, F, Wirtz, M, Schwaiger, M, and Wester, H.J.. First ^{18}F-labeled pentixafor-based imaging agent for PET imaging of CXCR4-expression in vivo. Tomography. 2016;2(2):85-93.

TOMOGRAPHY®

Andreas Poschenrieder, M.Sc.
PhD candidate
Chair of Pharmaceutical Radiochemistry
Faculties of Chemistry and Medicine
Technische Universität München
Walther-Meißner-Str. 3
85748 Garching

February 1, 2017

RE: Permission to use Figure

Dear Andreas,

I am writing to inform you that you have been approved for permission to use any and all parts of your article TOM-00130-16 entitled "First 18F-labeled pentixafor-based imaging agent for PET imaging of CXCR4-expression in vivo" (Tomography V2(2), 85, 2016 to republish in your Thesis.

Sincerely,

Brian D. Ross

Editor-in-Chief
Grapho Publications, Inc.

IV.3 Journal of Nuclear Medicine Publications

Hyafil F*, Pelisek J, Laitinen I, Schottelius M, Mohring M, Döring Y, Van der Vorst E, Kallmayer M, Steiger K, **Poschenrieder A**, et al., Imaging the cytokine receptor CXCR4 in atherosclerotic plaques with the radiotracer [^{68}Ga]pentixafor for positron emission tomography. J. Nucl. Med. 2017;58(3):499-506.

Herrmann K, Schottelius M, Lapa C, Osl T, **Poschenrieder A**, Hanscheid H et al. First-in-Human Experience of CXCR4-Directed Endoradiotherapy with ^{177}Lu and ^{90}Y-Labeled Pentixather in Advanced-Stage Multiple Myeloma with Extensive Intra- and Extramedullary Disease. J Nucl Med. 2016;57(2):248-51.

J Nucl Med.

Prof. Dr. Dominique Delbeke
Vanderbilt University Medical Center
Nashville, Tennessee, USA

Andreas Poschenrieder

[redacted]
81673 München
Mobil: [redacted]
Email:
a.poschenrieder@tum.de

München, 04.Nov.2016

Reuse/ Republication of the Entire Work in Theses or Collections

Dear Sir or Madam,

in order to satisfy the criteria of my degree-granting institution (Technische Universität München), I need a written confirmation that I may reuse the following publications for my dissertation.

Herrmann K, Schottelius M, Lapa C, Osl T, Poschenrieder A, Hanscheid H et al. First-in-Human Experience of CXCR4-Directed Endoradiotherapy with Lu-177- and Y-90-Labeled Pentixather in Advanced-Stage Multiple Myeloma with Extensive Intra- and Extramedullary Disease. J Nucl Med. 2016;57(2):248-51. doi:10.2967/jnumed.115.167361.

Hyafil F, Pelisek J, Laitinen I, Schottelius M, Mohring M, Doring Y et al. Imaging the cytokine receptor CXCR4 in atherosclerotic plaques with the radiotracer 68Ga-pentixafor for positron emission tomography. J Nucl Med. 2016. doi:10.2967/jnumed.116.179663.

By signing this form, you grant me confirmation, that the above stated work may be reused with appropriate citation to meet the criteria of my institution for submission of my dissertation.

Sincerely,

PhD Candidate
Andreas Poschenrieder
04.Nov.2016

Digitally signed by Mark Sumimoto
Date: 2016.11.11 15:30:56 -05'00'

J Nucl Med.
Person in charge
04.Nov.2016

IV.4 Elsevier Publications

Schottelius M, Konrad M, Osl T, **Poschenrieder A**, Wester H-J. An optimized strategy for the mild and efficient solution phase iodination of tyrosine residues in bioactive peptides. Tetrahedron Lett. 2015;56(47):6602-5.

ELSEVIER LICENSE TERMS AND CONDITIONS

This Agreement between Andreas Poschenrieder ("You") and Elsevier ("Elsevier") consists of your license details and the terms and conditions provided by Elsevier and Copyright Clearance Center.

Jan 17, 2017

License Number 3981990393073
License date Nov 04, 2016
Licensed Content Publisher Elsevier
Licensed Content Publication Tetrahedron Letters
Licensed Content Title An optimized strategy for the mild and efficient solution phase iodination of tyrosine residues in bioactive peptides
Licensed Content Author Margret Schottelius, Matthias Konrad, Theresa Osl, Andreas Poschenrieder, Hans-Jürgen Wester
Licensed Content Date 25 November 2015
Licensed Content Volume Number 56
Licensed Content Issue Number 47
Licensed Content Pages 4
Start Page 6602
End Page 6605
Type of Use reuse in a thesis/dissertation
Portion full article
Format both print and electronic
Are you the author of this Elsevier article? Yes
Will you be translating? No
Order reference number
Title of your thesis/dissertation Development of Diagnostic and Therapeutic Radiopharmaceuticals targeting the Chemokine Receptor CXCR4
Expected completion date Dec 2016
Estimated size (number of pages) 120

Elsevier VAT number GB 494 6272 12
Requestor Location Andreas Poschenrieder, Walther-Meißner Str.3, Garching, 85748 Germany, Attn: Andreas Poschenrieder
Total 0.00 EUR
Terms and Conditions: Special Rightsholder Terms & Conditions are available at: https://www.copyright.com/reviewCoiTermsConfirm.do?confirmNum=10673893

[…] Theses and dissertations which contain embedded published journal articles (PJAs) as part of the formal submission can be posted publicly by the awarding institution with DOI links back to the formal publications on ScienceDirect. If you are affiliated with a library that subscribes to ScienceDirect you have additional private sharing rights for others' research accessed under that agreement. This includes use for classroom teaching and internal training at the institution (including use in course packs and courseware programs), and inclusion of the article for grant funding purposes […].

Thesis/Dissertation: If your license is for use in a thesis/dissertation your thesis may be submitted to your institution in either print or electronic form. Should your thesis be published commercially, please reapply for permission. These requirements include permission for the Library and Archives of Canada to supply single copies, on demand, of the complete thesis and include permission for Proquest/UMI to supply single copies, on demand, of the complete thesis. Should your thesis be published commercially, please reapply for permission. Theses and dissertations which contain embedded PJAs as part of the formal submission can be posted publicly by the awarding institution with DOI links back to the formal publications on ScienceDirect.

IV.5 Theranostics Publications

Schottelius M*, Osl T, **Poschenrieder A**, Hoffmann F, Beykan S, Hänscheid H, Franke K, et al., [^{177}Lu]pentixather: comprehensive preclinical evaluation of a first CXCR4-directed endoradiotherapeutic agent. Theranostics. 2017;7(9):2350-2362.

An author or co-author of an article published in Theranostics is free to include or reuse the materials in other articles or theses or other publications with citation of the original source. Permission is automatically granted. Articles in Theranostics are distributed under the Creative Commons Attribution-NonCommercial 4.0 International License, as also explained in Chapter IV.1.

V. Summary and Outlook

In developed countries, cancer is the second leading cause of death, being only surpassed by cardiovascular diseases. CXCR4 and its only endogenous ligand CXCL12 are fundamentally involved in both of the diseases.

In physiology, the CXCR4/CXCL12 axis regulates the chemotaxis of stem and immune cells, being fundamentally involved in cell adhesion, proliferation and survival, as well as hematopoiesis, organogenesis, and tissue regeneration. In pathology, CXCR4 plays a critical role in the HIV-1 entry into target cells, inflammation, and myocardial infarction. Moreover, in oncology, CXCR4 is overexpressed and fundamentally involved in tumor growth and tissue specific metastasis to organs expressing abundant levels of CXCL12, as well as inflammation and myocardial infarction. Consequently, CXCR4 represents an important molecular target for tracer development aiming towards better patient management and personalized medicine. However, non-invasive CXCR4-targeting imaging agents and tracers for PRRT remain to be clinically transferred. Main objective of the presented thesis was therefore the development of CXCR4-targeted diagnostic and therapeutic radiopharmaceuticals.

Based on the successful CXCR4-targeting properties of [^{68}Ga]pentixafor as PET imaging agent of CXCR4 expression *in vitro* and *in vivo*, the cyclopentapeptide core of pentixafor *cyclo*(Gly-L-2-Nal-L-Arg-D-Orn-D-tyr) was used for further evaluations throughout the thesis. To broaden the spectrum of applicable radio(metal)-labeled pentixafor analogs for diagnostic and also therapeutic purposes, different chelators have been coupled to the pentapeptide and labeled with Ga^{3+}, AlF^{2+}, Zr^{4+}, Cu^{2+}, In^{3+}, Y^{3+}, Lu^{3+}, and Bi^{3+} relevant for medical applications. It has been shown that the binding affinity of pentixafor derivatives towards CXCR4 was greatly influenced by chelator and metal exchange. Within 30 metal-free or metal-labeled synthesized analogs, two new conjugates with an improved affinity compared to the parental compound [^{68}Ga]pentixafor have been identified, namely [^{nat}Ga]NOTA-pentixafor and [^{nat}Bi]DOTA-pentixafor.

[^{68}Ga]NOTA-pentixafor was preclinical evaluated as a PET imaging agent for CXCR4 expression *in vivo* and compared to [^{68}Ga]pentixafor. The study outlined the excellent CXCR4 targeting characteristics of [^{68}Ga]pentixafor and showed no advantages of [^{68}Ga]NOTA-pentixafor over [^{68}Ga]pentixafor.

In another study, [^{68}Ga]pentixafor was evaluated as potential PET imaging agent for CXCR4

expression in atherosclerotic plaques. The potential role of [^{68}Ga]pentixafor as a more specific PET imaging agent than FDG for the detection of CXCR4 expression in macrophage-infiltrating atherosclerotic plaques has been demonstrated.

Moreover, a method for the rapid and mild (mono)iodination of tyrosine residues of unprotected peptide precursors is presented. Iodination of pentixafor, giving pentixather, resulted in an enhanced affinity towards CXCR4 and higher flexibility towards structural modifications.

Major findings, using the penixather scaffold, included two promising imaging agents for CXCR4 expression *in vivo* and the first endoradiotherapeutic agent available for CXCR4-targeted therapy. [^{18}F]AlF-NOTA-pentixather and [^{64}Cu]NOTA-pentixather have been developed as promising PET tracers for imaging of CXCR4 expression. Both analogs were preclinically evaluated in a lymphoma xenograft and, although demonstrating higher uptake in excretory organs compared to [^{68}Ga]pentixafor, both tracers showed efficient CXCR4 targeting and clear delineation of the tumors.

In addition, the first CXCR4-directed endoradiotherapeutic agent, [^{177}Lu/^{90}Y]pentixather was developed. [^{177}Lu]pentixather demonstrated a suitable pharmacokinetic profile and specific targeting of CXCR4-positive cancer cells with high tumor accumulation and retention. Combined with an overall favorable dosimetry, enabling high radiation doses during PRRT, ^{177}Lu/^{90}Y-labeled pentixather was used in first clinical trials in patients with advanced-stage multiple myeloma and resulted in a remarkable therapeutic effect in two patients. Combined with [^{68}Ga]pentixafor as imaging agent, [^{177}Lu]pentixather is believed to offer high clinical potential for the endoradiotherapy of CXCR4-overexpressing malignancies, following a CXCR4-targeted theranostic concept towards individualized cancer therapies.

VI. References

1. Zlotnik A, Burkhardt AM, Homey B. Homeostatic chemokine receptors and organ-specific metastasis. *Nat Rev Immunol.* 2011;11:597-606.

2. Domanska UM, Kruizinga RC, Nagengast WB, et al. A review on CXCR4/CXCL12 axis in oncology: No place to hide. *European Journal of Cancer.* 2013;49:219-230.

3. Jacobson O, Weiss ID. CXCR4 Chemokine Receptor Overview: Biology, Pathology and Applications in Imaging and Therapy. *Theranostics.* 2013;3:1-2.

4. Zou YR, Kottmann AH, Kuroda M, Taniuchi I, Littman DR. Function of the chemokine receptor CXCR4 in haematopoiesis and in cerebellar development. *Nature.* 1998;393:595-599.

5. Ma Q, Jones D, Borghesani PR, et al. Impaired B-lymphopoiesis, myelopoiesis, and derailed cerebellar neuron migration in CXCR4- and SDF-1-deficient mice. *Proceedings of the National Academy of Sciences of the United States of America.* 1998;95:9448-9453.

6. Ara T, Nakamura Y, Egawa T, et al. Impaired colonization of the gonads by primordial germ cells in mice lacking a chemokine, stromal cell-derived factor-1 (SDF-1). *Proc Natl Acad Sci U S A.* 2003;100:5319-5323.

7. Müller A, Homey B, Soto H, et al. Involvement of chemokine receptors in breast cancer metastasis. *Nature.* 2001;410.

8. Burger JA, Kipps TJ. CXCR4: a key receptor in the crosstalk between tumor cells and their microenvironment. *Blood.* 2006;107.

9. Burger JA, Peled A. CXCR4 antagonists: targeting the microenvironment in leukemia and other cancers. *Leukemia.* 2009;23:43-52.

10. Cojoc M, Peitzsch C, Trautmann F, Polishchuk L, Telegeev GD, Dubrovska A. Emerging targets in cancer management: role of the CXCL12/CXCR4 axis. *Onco Targets Ther.* 2013;6:1347-1361.

11. Balkwill F. The significance of cancer cell expression of the chemokine receptor CXCR4. *Seminars in Cancer Biology.* 2004;14:171-179.

12. Weilbaecher KN, Guise TA, McCauley LK. Cancer to bone: a fatal attraction. *Nat Rev Cancer.* 2011;11:411-425.

13. Teicher BA, Fricker SP. CXCL12 (SDF-1)/CXCR4 Pathway in Cancer. *Clinical Cancer Research.* 2010;16:2927.

14. Balkwill F. Cancer and the chemokine network. *Nat Rev Cancer.* 2004;4:540-550.

15. Duda DG, Kozin SV, Kirkpatrick ND, Xu L, Fukumura D, Jain RK. CXCL12 (SDF1α) – CXCR4/CXCR7 Pathway Inhibition: An Emerging Sensitizer for Anti-Cancer Therapies?

Clinical cancer research : an official journal of the American Association for Cancer Research. 2011;17:2074-2080.

16. Guo F, Wang Y, Liu J, Mok SC, Xue F, Zhang W. CXCL12/CXCR4: a symbiotic bridge linking cancer cells and their stromal neighbors in oncogenic communication networks. *Oncogene.* 2016;35:816-826.

17. Wu T, Dai Y. Tumor microenvironment and therapeutic response. *Cancer Lett.* 2016.

18. Woodard LE, Nimmagadda S. CXCR4-based imaging agents. *J Nucl Med.* 2011;52:1665-1669.

19. Liang JJ, Zhu S, Bruggeman R, et al. High levels of expression of human stromal cell-derived factor-1 are associated with worse prognosis in patients with stage II pancreatic ductal adenocarcinoma. *Cancer Epidemiol Biomarkers Prev.* 2010;19:2598-2604.

20. Guo L, Cui ZM, Zhang J, Huang Y. Chemokine axes CXCL12/CXCR4 and CXCL16/CXCR6 correlate with lymph node metastasis in epithelial ovarian carcinoma. *Chin J Cancer.* 2011;30:336-343.

21. Barbolina MV, Kim M, Liu Y, et al. Microenvironmental Regulation of Chemokine (C-X-C-Motif) Receptor 4 in Ovarian Carcinoma. *Molecular Cancer Research.* 2010;8:653.

22. Burger JA, Kipps TJ. CXCR4: a key receptor in the crosstalk between tumor cells and their microenvironment. *Blood.* 2006;107:1761-1767.

23. Zhu L, Zhao Q, Wu B. Structure-based studies of chemokine receptors. *Curr Opin Struct Biol.* 2013;23:539-546.

24. Wu B, Chien E, Mol C, Fenalti G. Structures of the CXCR4 chemokine receptor in complex with small molecule and cyclic peptide antagonists. *Science.* 2010;330:1066-1071.

25. Yoshikawa Y, Kobayashi K, Oishi S, Fujii N, Furuya T. Molecular modeling study of cyclic pentapeptide CXCR4 antagonists: New insight into CXCR4-FC131 interactions. *Bioorganic & Medicinal Chemistry Letters.* 2012;22:2146-2150.

26. Demmer O, Frank AO, Hagn F, et al. A conformationally frozen peptoid boosts CXCR4 affinity and anti-HIV activity. *Angew Chem Int Ed Engl.* 2012;51:8110-8113.

27. Demmer O, Dijkgraaf I, Schumacher U, Marinelli L, Cosconati S, Gourni E. Design, synthesis, and functionalization of dimeric peptides targeting chemokine receptor CXCR4. *J Med Chem.* 2011;54.

28. Vabeno J, Nikiforovich GV, Marshall GR. Insight into the binding mode for cyclopentapeptide antagonists of the CXCR4 receptor. *Chem Biol Drug Des.* 2006;67:346-354.

29. Fujii N, Oishi S, Hiramatsu K, Araki T, Ueda S, Tamamura H. Molecular-size reduction of a potent CXCR4-chemokine antagonist using orthogonal combination of conformation- and sequence-based libraries. *Angew Chem.* 2003;42.

30. Masuda M, Nakashima H, Ueda T, et al. A novel anti-HIV synthetic peptide, T-22 ([Tyr5,12,Lys7]-polyphemusin II). *Biochem Biophys Res Commun.* 1992;189:845-850.

31. Tamamura H, Waki M, Imai M, et al. Downsizing of an HIV-cell fusion inhibitor, T22 ([Tyr5,12, Lys7]-polyphemusin II), with the maintenance of anti-HIV activity and solution structure. *Bioorg Med Chem.* 1998;6:473-479.

32. Tamamura H, Omagari A, Oishi S, et al. Pharmacophore identification of a specific CXCR4 inhibitor, T140, leads to development of effective anti-HIV agents with very high selectivity indexes. *Bioorg Med Chem Lett.* 2000;10:2633-2637.

33. Haubner R, Kuhnast B, Mang C, et al. [18F]Galacto-RGD: synthesis, radiolabeling, metabolic stability, and radiation dose estimates. *Bioconjug Chem.* 2004;15:61-69.

34. Mungalpara J, Thiele S, Eriksen O, Eksteen J, Rosenkilde MM, Vabeno J. Rational Design of Conformationally Constrained Cyclopentapeptide Antagonists for C-X-C Chemokine Receptor 4 (CXCR4). *Journal of Medicinal Chemistry.* 2012;55:10287-10291.

35. Mungalpara J, Zachariassen ZG, Thiele S, Rosenkilde MM, Vabeno J. Structure-activity relationship studies of the aromatic positions in cyclopentapeptide CXCR4 antagonists. *Org Biomol Chem.* 2013.

36. Demmer O, Gourni E, Schumacher U, Kessler H, Wester HJ. PET Imaging of CXCR4 Receptors in Cancer by a New Optimized Ligand. *Chemmedchem.* 2011;6:1789-1791.

37. Gourni E, Demmer O, Schottelius M, et al. PET of CXCR4 expression by a (68)Ga-labeled highly specific targeted contrast agent. *J Nucl Med.* 2011;52:1803-1810.

38. Feng Y, Broder CC, Kennedy PE, Berger EA. HIV-1 entry cofactor: Functional cDNA cloning of a seven-transmembrane, G protein-coupled receptor. *Science.* 1996;272:872-877.

39. Bleul CC, Farzan M, Choe H, et al. The lymphocyte chemoattractant SDF-1 is a ligand for LESTR/fusin and blocks HIV-1 entry. *Nature.* 1996;382:829-833.

40. Hanaoka H, Mukai T, Tamamura H, et al. Development of a 111In-labeled peptide derivative targeting a chemokine receptor, CXCR4, for imaging tumors. *Nucl Med Biol.* 2006;33:489-494.

41. De Clercq E. The bicyclam AMD3100 story. *Nat Rev Drug Discov.* 2003;2:581-587.

42. Tamamura H, Xu Y, Hattori T, et al. A low-molecular-weight inhibitor against the chemokine receptor CXCR4: a strong anti-HIV peptide T140. *Biochem Biophys Res Commun.* 1998;253:877-882.

43. Doranz BJ, Grovit-Ferbas K, Sharron MP, et al. A small-molecule inhibitor directed against the chemokine receptor CXCR4 prevents its use as an HIV-1 coreceptor. *J Exp Med.* 1997;186:1395-1400.

44. Hendrix CW, Flexner C, MacFarland RT, et al. Pharmacokinetics and safety of AMD-3100, a novel antagonist of the CXCR-4 chemokine receptor, in human volunteers. *Antimicrob Agents Chemother.* 2000;44:1667-1673.

45. Brave M, Farrell A, Ching Lin S, et al. FDA review summary: Mozobil in combination with granulocyte colony-stimulating factor to mobilize hematopoietic stem cells to the peripheral blood for collection and subsequent autologous transplantation. *Oncology.* 2010;78:282-288.

46. Tavor S, Eisenbach M, Jacob-Hirsch J, et al. The CXCR4 antagonist AMD3100 impairs survival of human AML cells and induces their differentiation. *Leukemia.* 2008;22:2151-5158.

47. Nervi B, Ramirez P, Rettig MP, et al. Chemosensitization of acute myeloid leukemia (AML) following mobilization by the CXCR4 antagonist AMD3100. *Blood.* 2009;113:6206-6214.

48. Burger JA, Stewart DJ, Wald O, Peled A. Potential of CXCR4 antagonists for the treatment of metastatic lung cancer. *Expert Review of Anticancer Therapy.* 2011;11:621-630.

49. Liang X. CXCR4, inhibitors and mechanisms of action. *Chem Biol Drug Des.* 2008;72:97-110.

50. Patrussi L, Baldari CT. The CXCL12/CXCR4 Axis as a Therapeutic Target in Cancer and HIV-1 Infection. *Current Medicinal Chemistry.* 2011;18:497-512.

51. Peled A, Wald O, Burger J. Development of novel CXCR4-based therapeutics. *Expert Opin Investig Drugs.* 2012;21:341-353.

52. Singh IP, Chauthe SK. Small molecule HIV entry inhibitors: Part I. Chemokine receptor antagonists: 2004 – 2010. *Expert Opinion on Therapeutic Patents.* 2011;21:227-269.

53. Wong D, Korz W. Translating an Antagonist of Chemokine Receptor CXCR4: From Bench to Bedside. *Clinical Cancer Research.* 2008;14:7975.

54. Choi WT, Duggineni S, Xu Y, Huang ZW, An J. Drug Discovery Research Targeting the CXC Chemokine Receptor 4 (CXCR4). *Journal of Medicinal Chemistry.* 2012;55:977-994.

55. Oishi S, Fujii N. Peptide and peptidomimetic ligands for CXC chemokine receptor 4 (CXCR4). *Organic & Biomolecular Chemistry.* 2012;10:5720-5731.

56. Koglin N, Anton M, Hauser A, et al. CXCR4 chemokine receptor SPECT/PET imaging with radiolabeled CPCR4: A promising approach for imaging metastatic processes. *Journal of Nuclear Medicine.* 2006;47:505P.

57. Jacobson O, Weiss ID, Kiesewetter DO, Farber JM, Chen XY. PET of Tumor CXCR4 Expression with 4-F-18-T140. *Journal of Nuclear Medicine.* 2010;51:1796-1804.

58. Poty S, Desogere P, Goze C, et al. New AMD3100 derivatives for CXCR4 chemokine receptor targeted molecular imaging studies: synthesis, anti-HIV-1 evaluation and binding affinities. *Dalton Transactions.* 2015;44:5004-5016.

59. Aghanejad A, Jalilian AR, Fazaeli Y, et al. Synthesis and Evaluation of [(67)Ga]-AMD3100: A Novel Imaging Agent for Targeting the Chemokine Receptor CXCR4. *Sci Pharm.* 2014;82:29-42.

60. Hartimath SV, Domanska UM, Walenkamp AME, Rudi A.J.O D, de Vries EFJ. [99mTc]O2-AMD3100 as a SPECT tracer for CXCR4 receptor imaging. *Nuclear Medicine and Biology.* 2013;40:507-517.

61. Liang ZX, Zhan WQ, Zhu AZ, et al. Development of a Unique Small Molecule Modulator of CXCR4. *Plos One.* 2012;7.

62. Shim H, Liotta DC, Zhu A, Goodman M. Cxcr4 antagonists for imaging of cancer and inflammatory disorders. Google Patents; 2011.

63. Zhang JM, Tian JH, Li TR, Guo HY, Shen L. 99mTc–AMD3100: A novel potential receptor-targeting radiopharmaceutical for tumor imaging. *Chinese Chemical Letters.* 2010;21:461-463.

64. Weiss ID, Jacobson O, Kiesewetter DO, et al. Positron emission tomography imaging of tumors expressing the human chemokine receptor CXCR4 in mice with the use of 64Cu-AMD3100. *Mol Imaging Biol.* 2012;14:106-114.

65. De Silva RA, Peyre K, Pullambhatla M, Fox JJ, Pomper MG, Nimmagadda S. Imaging CXCR4 expression in human cancer xenografts: evaluation of monocyclam 64Cu-AMD3465. *J Nucl Med.* 2011;52:986-993.

66. Nimmagadda S, Pullambhatla M, Stone K, Green G, Bhujwalla ZM, Pomper MG. Molecular imaging of CXCR4 receptor expression in human cancer xenografts with [64Cu]AMD3100 positron emission tomography. *Cancer Res.* 2010;70:3935-3944.

67. Jacobson O, Weiss ID, Szajek L, Farber JM, Kiesewetter DO. 64Cu-AMD3100--a novel imaging agent for targeting chemokine receptor CXCR4. *Bioorg Med Chem.* 2009;17:1486-1493.

68. Khan A, Silversides JD, Madden L, Greenman J, Archibald SJ. Fluorescent CXCR4 chemokine receptor antagonists: metal activated binding. *Chem Commun (Camb).* 2007:416-418.

69. Woodard LE, De Silva RA, Behnam Azad B, et al. Bridged cyclams as imaging agents for chemokine receptor 4 (CXCR4). *Nucl Med Biol.* 2014;41:552-561.

70. Oltmanns D, Zitzmann-Kolbe S, Mueller A, et al. Zn(II)-bis(cyclen) complexes and the imaging of apoptosis/necrosis. *Bioconjug Chem.* 2011;22:2611-2624.

71. Hartimath SV, van Waarde A, Dierckx RA, de Vries EF. Evaluation of N-[(11)C]methyl-AMD3465 as a PET tracer for imaging of CXCR4 receptor expression in a C6 glioma tumor model. *Mol Pharm.* 2014;11:3810-3817.

72. Poty S, Gourni E, Desogere P, et al. AMD3100: A Versatile Platform for CXCR4 Targeting (68)Ga-Based Radiopharmaceuticals. *Bioconjug Chem.* 2016;27:752-761.

73. Yan X, Niu G, Wang Z, et al. Al[F]NOTA-T140 Peptide for Noninvasive Visualization of CXCR4 Expression. *Mol Imaging Biol.* 2015.

74. Zhang XX, Sun Z, Guo J, et al. Comparison of (18)F-labeled CXCR4 antagonist peptides for PET imaging of CXCR4 expression. *Mol Imaging Biol.* 2013;15:758-767.

75. Jacobson O, Weiss ID, Szajek LP, et al. Improvement of CXCR4 tracer specificity for PET imaging. *J Control Release.* 2012;157:216-223.

76. Jacobson O, Weiss ID, Szajek LP, et al. PET imaging of CXCR4 using copper-64 labeled peptide antagonist. *Theranostics.* 2011;1:251-262.

77. Hennrich U, Seyler L, Schafer M, et al. Synthesis and in vitro evaluation of 68Ga-DOTA-4-FBn-TN14003, a novel tracer for the imaging of CXCR4 expression. *Bioorg Med Chem.* 2012;20:1502-1510.

78. Kuil J, Buckle T, Yuan H, et al. Synthesis and Evaluation of a Bimodal CXCR4 Antagonistic Peptide. *Bioconjugate Chemistry.* 2011;22:859-864.

79. Kuil J, Buckle T, Oldenburg J, et al. Hybrid peptide dendrimers for imaging of chemokine receptor 4 (CXCR4) expression. *Mol Pharm.* 2011;8:2444-2453.

80. Nishizawa K, Nishiyama H, Oishi S, et al. Fluorescent imaging of high-grade bladder cancer using a specific antagonist for chemokine receptor CXCR4. *Int J Cancer.* 2010;127:1180-1187.

81. Demmer O, Dijkgraaf I, Schumacher U, et al. Design, Synthesis, and Functionalization of Dimeric Peptides Targeting Chemokine Receptor CXCR4. *Journal of Medicinal Chemistry.* 2011;54:7648-7662.

82. Tanaka T, Nomura W, Narumi T, Masuda A, Tamamura H. Bivalent ligands of CXCR4 with rigid linkers for elucidation of the dimerization state in cells. *J Am Chem Soc.* 2010;132:15899-15901.

83. Poschenrieder A, Osl T, Schottelius M, et al. First 18F-Labeled Pentixafor-Based Imaging Agent for PET Imaging of CXCR4 Expression In Vivo. *Tomography.* 2016;2:85-93.

84. Kuil J, Buckle T, van Leeuwen FW. Imaging agents for the chemokine receptor 4 (CXCR4). *Chem Soc Rev.* 2012;41:5239-5261.

85. Debnath B, Xu S, Grande F, Garofalo A, Neamati N. Small molecule inhibitors of CXCR4. *Theranostics.* 2013;3:47-75.

86. Weiss ID, Jacobson O. Molecular imaging of chemokine receptor CXCR4. *Theranostics.* 2013;3:76-84.

87. Charron CL, Hickey JL, Nsiama TK, Cruickshank DR, Turnbull WL, Luyt LG. Molecular imaging probes derived from natural peptides. *Natural Product Reports.* 2016;33:761-800.

88. Herrmann K, Lapa C, Wester HJ, et al. Biodistribution and radiation dosimetry for the chemokine receptor CXCR4-targeting probe 68Ga-pentixafor. *J Nucl Med.* 2015;56:410-416.

89. Wester HJ, Keller U, Schottelius M, et al. Disclosing the CXCR4 Expression in Lymphoproliferative Diseases by Targeted Molecular Imaging. *Theranostics.* 2015;5:618-630.

90. Herhaus P, Habringer S, Philipp-Abbrederis K, et al. Targeted positron emission tomography imaging of CXCR4 expression in patients with acute myeloid leukemia. *Haematologica.* 2016;101:932-940.

91. Lapa C, Schreder M, Schirbel A, et al. [68Ga]Pentixafor-PET/CT for imaging of chemokine receptor CXCR4 expression in multiple myeloma - Comparison to [18F]FDG and laboratory values. *Theranostics.* 2017;7:205-212.

92. Philipp-Abbrederis K, Herrmann K, Knop S, et al. In vivo molecular imaging of chemokine receptor CXCR4 expression in patients with advanced multiple myeloma. *EMBO Mol Med.* 2015;7:477-487.

93. Bluemel C, Hahner S, Heinze B, et al. Investigating the Chemokine Receptor 4 as Potential Theranostic Target in Adrenocortical Cancer Patients. *Clin Nucl Med.* 2016.

94. Lapa C, Luckerath K, Kleinlein I, et al. (68)Ga-Pentixafor-PET/CT for Imaging of Chemokine Receptor 4 Expression in Glioblastoma. *Theranostics.* 2016;6:428-434.

95. Lapa C, Luckerath K, Rudelius M, et al. [68Ga]Pentixafor-PET/CT for imaging of chemokine receptor 4 expression in small cell lung cancer - initial experience. *Oncotarget.* 2016.

96. Vag T, Gerngross C, Herhaus P, et al. First Experience with Chemokine Receptor CXCR4-Targeted PET Imaging of Patients with Solid Cancers. *J Nucl Med.* 2016;57:741-746.

97. Hyafil F, Pelisek J, Laitinen I, et al. Imaging the Cytokine Receptor CXCR4 in Atherosclerotic Plaques with the Radiotracer 68Ga-Pentixafor for PET. *Journal of Nuclear Medicine.* 2017;58:499-506.

98. Lapa C, Reiter T, Werner RA, et al. [(68)Ga]Pentixafor-PET/CT for Imaging of Chemokine Receptor 4 Expression After Myocardial Infarction. *JACC Cardiovasc Imaging.* 2015;8:1466-1468.

99. Thackeray JT, Derlin T, Haghikia A, et al. Molecular Imaging of the Chemokine Receptor CXCR4 After Acute Myocardial Infarction. *JACC Cardiovasc Imaging.* 2015;8:1417-1426.

100. Rischpler C, Nekolla SG, Kossmann H, et al. Upregulated myocardial CXCR4-expression after myocardial infarction assessed by simultaneous GA-68 pentixafor PET/MRI. *J Nucl Cardiol.* 2016;23:131-133.

101. Schmid JS, Schirbel A, Buck AK, Kropf S, Wester HJ, Lapa C. [68Ga]Pentixafor-Positron Emission Tomography/Computed Tomography Detects Chemokine Receptor CXCR4 Expression After Ischemic Stroke. *Circ Cardiovasc Imaging.* 2016;9:e005217.

102. Wester HJ, Keller U, Schottelius M, Beer A, Philipp-Abbrederis K, Hoffmann F. Disclosing the CXCR4 expression in lymphoproliferative diseases by targeted molecular imaging. *Theranostics.* 2015;5.

103. Poschenrieder Andreas, Schottelius Margret, Weineisen Martina, et al. First F-18-labeled pentixafor-based imaging agent for high-contrast PET imaging of CXCR4-expression in vivo. *Nuklearmedizin (DGN).* 2015;54:A15.

104. Price EW, Orvig C. Matching chelators to radiometals for radiopharmaceuticals. *Chem Soc Rev.* 2014;43:260-290.

105. Liu S. Bifunctional coupling agents for radiolabeling of biomolecules and target-specific delivery of metallic radionuclides. *Adv Drug Deliv Rev.* 2008;60:1347-1370.

106. Bartholomä MD. Recent developments in the design of bifunctional chelators for metal-based radiopharmaceuticals used in Positron Emission Tomography. *Inorganica Chimica Acta.* 2012;389:36-51.

107. Zeglis BM, Lewis JS. A practical guide to the construction of radiometallated bioconjugates for positron emission tomography. *Dalton Transactions.* 2011;40:6168-6195.

108. Wadas TJ, Wong EH, Weisman GR, Anderson CJ. Coordinating Radiometals of Copper, Gallium, Indium, Yttrium, and Zirconium for PET and SPECT Imaging of Disease. *Chemical Reviews.* 2010;110:2858-2902.

109. Brasse D, Nonat A. Radiometals: towards a new success story in nuclear imaging? *Dalton Trans.* 2015;44:4845-4858.

110. Kukis DL, Diril H, Greiner DP, et al. A comparative study of copper-67 radiolabeling and kinetic stabilities of antibody-macrocycle chelate conjugates. *Cancer.* 1994;73:779-786.

111. Bass LA, Wang M, Welch MJ, Anderson CJ. In vivo transchelation of copper-64 from TETA-octreotide to superoxide dismutase in rat liver. *Bioconjug Chem.* 2000;11:527-532.

112. Cooper MS, Ma MT, Sunassee K, et al. Comparison of (64)Cu-complexing bifunctional chelators for radioimmunoconjugation: labeling efficiency, specific activity, and in vitro/in vivo stability. *Bioconjug Chem.* 2012;23:1029-1039.

113. Stasiuk GJ, Long NJ. The ubiquitous DOTA and its derivatives: the impact of 1,4,7,10-tetraazacyclododecane-1,4,7,10-tetraacetic acid on biomedical imaging. *Chem Commun (Camb).* 2013;49:2732-2746.

114. Cutler CS, Hennkens HM, Sisay N, Huclier-Markai S, Jurisson SS. Radiometals for combined imaging and therapy. *Chem Rev.* 2013;113:858-883.

115. McBride WJ, Sharkey RM, Goldenberg DM. Radiofluorination using aluminum-fluoride (Al18F). *EJNMMI Res.* 2013;3:36.

116. Martin RB. Ternary complexes of Al3+ and F- with a third ligand. *Coordination Chemistry Reviews.* 1996;141:23-32.

117. Mirick GR, O'Donnell RT, DeNardo SJ, Shen S, Meares CF, DeNardo GL. Transfer of copper from a chelated 67Cu-antibody conjugate to ceruloplasmin in lymphoma patients. *Nucl Med Biol.* 1999;26:841-845.

118. Ferreira CL, Lamsa E, Woods M, et al. Evaluation of Bifunctional Chelates for the Development of Gallium-Based Radiopharmaceuticals. *Bioconjugate Chemistry.* 2010;21:531-536.

119. Vallabhajosula S. Chapter 6 - PET and SPECT Scanners. *Springer.* 2009:59-81.

120. Cherry SR, Sorenson JA, Phelps ME. chapter 4 - Decay of Radioactivity. *Physics in Nuclear Medicine (Fourth Edition)*. Philadelphia: W.B. Saunders; 2012:31-42.

121. Magill JP, Galy J. Karlsruher Nuklidkarte. *In: Communities E, editor.* 2006-2009.

122. Rahmim A, Zaidi H. PET versus SPECT: strengths, limitations and challenges. *Nucl Med Commun* 2008;29:193-207.

123. van der Have F, Vastenhouw B, Ramakers RM, et al. U-SPECT-II: An Ultra-High-Resolution Device for Molecular Small-Animal Imaging. *J Nucl Med.* 2009;50:599-605.

124. Haralampieva DG, Ametamey SM, Sulser T, Eberli D. Non-Invasive Imaging Modalities for Clinical Investigation in Regenerative Medicine, Cells and Biomaterials in Regenerative Medicine. *InTech.* 2014.

125. Cherry SR, Sorenson JA, Phelps ME. chapter 18 - Positron Emission Tomography. *Physics in Nuclear Medicine (Fourth Edition)*. Philadelphia: W.B. Saunders; 2012:307-343.

126. Chatziioannou A, Tai YC, Doshi N, Cherry SR. Detector development for microPET II: a 1 microl resolution PET scanner for small animal imaging. *Phys Med Biol.* 2001;46:2899-2910.

127. Yang Y, Tai YC, Siegel S, et al. Optimization and performance evaluation of the microPET II scanner for in vivo small-animal imaging. *Phys Med Biol.* 2004;49:2527-2545.

128. Conti M, Eriksson L. Physics of pure and non-pure positron emitters for PET: a review and a discussion. *EJNMMI Physics.* 2016;3:8.

129. Kuntner C, Stout D. Quantitative preclinical PET imaging: opportunities and challenges. *Frontiers in Physics.* 2014;2.

130. Levin CS, Hoffman EJ. Calculation of positron range and its effect on the fundamental limit of positron emission tomography system spatial resolution. *Phys Med Biol.* 1999;44:781-799.

131. Sanchez-Crespo A. Comparison of Gallium-68 and Fluorine-18 imaging characteristics in positron emission tomography. *Appl Radiat Isot.* 2013;76:55-62.

132. Sanchez-Crespo A, Andreo P, Larsson SA. Positron flight in human tissues and its influence on PET image spatial resolution. *Eur J Nucl Med Mol Imaging.* 2004;31:44-51.

133. Soderlund AT, Chaal J, Tjio G, Totman JJ, Conti M, Townsend DW. Beyond 18F-FDG: Characterization of PET/CT and PET/MR Scanners for a Comprehensive Set of Positron Emitters of Growing Application--18F, 11C, 89Zr, 124I, 68Ga, and 90Y. *J Nucl Med.* 2015;56:1285-1291.

134. Raylman RR, Hammer BE, Christensen NL. Combined MRI-PET scanner: a Monte Carlo evaluation of the improvements in PET resolution due to the effects of a static homogeneous magnetic field. *IEEE Trans Nucl Sci.* 1996;44:184-189.

135. George GP, Pisaneschi F, Nguyen QD, Aboagye EO. Positron emission tomographic imaging of CXCR4 in cancer: challenges and promises. *Mol Imaging.* 2014;13:1-19.

136. Nayak TR, Hong H, Zhang Y, Cai W. Multimodality Imaging of CXCR4 in Cancer: Current Status towards Clinical Translation. *Current Molecular Medicine.* 2013;13:1538-1548.

137. Masuda R, Oishi S, Ohno H, Kimura H, Saji H, Fujii N. Concise site-specific synthesis of DTPA-peptide conjugates: application to imaging probes for the chemokine receptor CXCR4. *Bioorg Med Chem.* 2011;19:3216-3220.

138. Nimmagadda S, Pullambhatla M, Pomper MG. Immunoimaging of CXCR4 expression in brain tumor xenografts using SPECT/CT. *J Nucl Med.* 2009;50:1124-1130.

139. Misra P, Lebeche D, Ly H, et al. Quantitation of CXCR4 expression in myocardial infarction using 99mTc-labeled SDF-1alpha. *J Nucl Med.* 2008;49:963-969.

140. George GP, Stevens E, Aberg O, et al. Preclinical evaluation of a CXCR4-specific (68)Ga-labelled TN14003 derivative for cancer PET imaging. *Bioorg Med Chem.* 2014;22:796-803.

141. Wang Z, Zhang M, Wang L, et al. Prospective Study of (68)Ga-NOTA-NFB: Radiation Dosimetry in Healthy Volunteers and First Application in Glioma Patients. *Theranostics.* 2015;5:882-889.

142. Sano K, Masuda R, Hisada H, et al. A radiogallium-DOTA-based bivalent peptidic ligand targeting a chemokine receptor, CXCR4, for tumor imaging. *Bioorg Med Chem Lett.* 2014;24:1386-1388.

143. Stigbrand T, Carlsson, Jorgen, Adams, Gregory P. Targeted Radionuclide Tumor Therapy - Biological Aspects. *Springer.* 2008.

144. Nicolas G, Giovacchini G, Muller-Brand J, Forrer F. Targeted radiotherapy with radiolabeled somatostatin analogs. *Endocrinol Metab Clin North Am.* 2011;40:187-204, ix-x.

145. Baldelli R, Barnabei A, Rizza L, et al. Somatostatin Analogs Therapy in Gastroenteropancreatic Neuroendocrine Tumors: Current Aspects and New Perspectives. *Frontiers in Endocrinology.* 2014;5:7.

146. Shah M, Da Silva R, Gravekamp C, Libutti SK, Abraham T, Dadachova E. Targeted radionuclide therapies for pancreatic cancer. *Cancer Gene Ther.* 2015;22:375-379.

147. de Jong M, Breeman WA, Valkema R, Bernard BF, Krenning EP. Combination radionuclide therapy using 177Lu- and 90Y-labeled somatostatin analogs. *J Nucl Med.* 2005;46 Suppl 1:13S-17S.

148. Kwekkeboom DJ, de Herder WW, Kam BL, et al. Treatment with the radiolabeled somatostatin analog [177 Lu-DOTA 0,Tyr3]octreotate: toxicity, efficacy, and survival. *J Clin Oncol.* 2008;26:2124-2130.

149. McDevitt MR, Sgouros G, Finn RD, et al. Radioimmunotherapy with alpha-emitting nuclides. *Eur J Nucl Med.* 1998;25:1341-1351.

150. Elgqvist J, Frost S, Pouget J-P, Albertsson P. The potential and hurdles of Targeted Alpha Therapy - Clinical trials and beyond. *Frontiers in Oncology.* 2014;3.

151. Friesen C, Glatting G, Koop B, et al. Breaking chemoresistance and radioresistance with [213Bi]anti-CD45 antibodies in leukemia cells. *Cancer Res.* 2007;67:1950-1958.

152. Hall EJ. *Radiobiology for the radiologist*. 5th ed. Philadelphia: Lippincott Williams & Wilkins; 2000.

153. Morgenstern A, Bruchertseifer F, Apostolidis C. Bismuth-213 and actinium-225 -- generator performance and evolving therapeutic applications of two generator-derived alpha-emitting radioisotopes. *Curr Radiopharm.* 2012;5:221-227.

154. Hassfjell S, Brechbiel MW. The development of the alpha-particle emitting radionuclides 212Bi and 213Bi, and their decay chain related radionuclides, for therapeutic applications. *Chem Rev.* 2001;101:2019-2036.

155. Press OW, Rasey J. Principles of radioimmunotherapy for hematologists and oncologists. *Semin Oncol.* 2000;27:62-73.

156. Press OW. Radioimmunotherapy for non-Hodgkin's lymphomas: a historical perspective. *Semin Oncol.* 2003;30:10-21.

157. Press OW, Shan D, Howell-Clark J, et al. Comparative metabolism and retention of iodine-125, yttrium-90, and indium-111 radioimmunoconjugates by cancer cells. *Cancer Res.* 1996;56:2123-2129.

158. Bakker WH, Breeman WA, van der Pluijm ME, de Jong M, Visser TJ, Krenning EP. Iodine-131 labelled octreotide: not an option for somatostatin receptor therapy. *Eur J Nucl Med.* 1996;23:775-781.

159. Mulligan T, Carrasquillo JA, Chung Y, et al. Phase I study of intravenous Lu-labeled CC49 murine monoclonal antibody in patients with advanced adenocarcinoma. *Clin Cancer Res.* 1995;1:1447-1454.

160. Alvarez RD, Partridge EE, Khazaeli MB, et al. Intraperitoneal radioimmunotherapy of ovarian cancer with 177Lu-CC49: a phase I/II study. *Gynecol Oncol.* 1997;65:94-101.

161. O'Donnell RT, DeNardo GL, Kukis DL, et al. A clinical trial of radioimmunotherapy with 67Cu-2IT-BAT-Lym-1 for non-Hodgkin's lymphoma. *J Nucl Med.* 1999;40:2014-2020.

162. Yeong CH, Cheng MH, Ng KH. Therapeutic radionuclides in nuclear medicine: current and future prospects. *J Zhejiang Univ Sci B.* 2014;15:845-863.

163. Fani M, Maecke HR, Okarvi SM. Radiolabeled peptides: valuable tools for the detection and treatment of cancer. *Theranostics.* 2012;2:481-501.

164. Gudkov SV, Shilyagina NY, Vodeneev VA, Zvyagin AV. Targeted Radionuclide Therapy of Human Tumors. *Int J Mol Sci.* 2015;17.

165. Chatterjee S, Azad BB, Nimmagadda S. The Intricate Role of CXCR4 in Cancer. *Emerging Applications of Molecular Imaging to Oncology.* 2014;124:31-82.

166. Schottelius M, Konrad M, Osl T, Poschenrieder A, Wester H-J. An optimized strategy for the mild and efficient solution phase iodination of tyrosine residues in bioactive peptides. *Tetrahedron Letters.* 2015;56:6602-6605.

167. Herrmann K, Schottelius M, Lapa C, et al. First-in-Human Experience of CXCR4-Directed Endoradiotherapy with 177Lu- and 90Y-Labeled Pentixather in Advanced-Stage Multiple Myeloma with Extensive Intra- and Extramedullary Disease. *J Nucl Med.* 2016;57:248-251.

168. Milenic DE, Brady ED, Brechbiel MW. Antibody-targeted radiation cancer therapy. *Nat Rev Drug Discov.* 2004;3:488-499.

169. Poschenrieder A, Schottelius M, Schwaiger M, Kessler H, Wester H-J. The influence of different metal-chelate conjugates of pentixafor on the CXCR4 affinity. *EJNMMI Research.* 2016;6:1-8.

170. de Sa A, Matias AA, Prata MI, Geraldes CF, Ferreira PM, Andre JP. Gallium labeled NOTA-based conjugates for peptide receptor-mediated medical imaging. *Bioorg Med Chem Lett.* 2010;20:7345-7348.

171. de Blois E, Chan HS, Breeman WA. Iodination and stability of somatostatin analogues: comparison of iodination techniques. A practical overview. *Curr Top Med Chem.* 2012;12:2668-2676.

172. McBride WJ, Sharkey RM, Karacay H, et al. A novel method of 18F radiolabeling for PET. *J Nucl Med.* 2009;50:991-998.

VII. Appendix

Appendix 1: **Poschenrieder A***, Schottelius M, Schwaiger M, Kessler H, Wester H-J. The influence of different metal-chelate conjugates of pentixafor on the CXCR4 affinity. EJNMMI research. 2016;6(1):1-8

Appendix 2: **Poschenrieder A***, Schottelius M, Schwaiger M, Wester H-J. Preclinical evaluation of [^{68}Ga]NOTA-pentixafor for PET imaging of CXCR4 expression *in vivo* - a comparison to [^{68}Ga]pentixafor. EJNMMIR. 2016;6(1):1-5.

Appendix 3: Schottelius M*, Konrad M, Osl T, **Poschenrieder A**, Wester H-J. An optimized strategy for the mild and efficient solution phase iodination of tyrosine residues in bioactive peptides. Tetrahedron Lett. 2015;56(47):6602-5.

Appendix 4: **Poschenrieder A***, Osl T, Schottelius M, Hoffmann F, Wirtz M, Schwaiger M, and Wester H.J.. First ^{18}F-labeled pentixafor-based imaging agent for PET imaging of CXCR4-expression *in vivo*. Tomography. 2016;2(2):85-93. **Highlighted on cover**

Appendix 5: **Poschenrieder A**, Schottelius M*, Osl T, Schwaiger M, Wester H-J. [^{64}Cu]NOTA-pentixather enables high resolution PET imaging of CXCR4 expression in a preclinical lymphoma model. EJNMMI Radiopharmacy and Chemistry. 2017;2:2.

Appendix 6: Schottelius M*, Osl T, **Poschenrieder A**, Hoffmann F, Beykan S, Hänscheid H, Franke K, et al., [^{177}Lu]pentixather: comprehensive preclinical evaluation of a first CXCR4-directed endoradiotherapeutic agent. Theranostics. 2017;7(9):2350-2362.

Appendix 7: Herrmann K*, Schottelius M, Lapa C, Osl T, **Poschenrieder A**, Hanscheid H et al. First-in-Human Experience of CXCR4-Directed Endoradiotherapy with ^{177}Lu and ^{90}Y-labeled Pentixather in Advanced-Stage Multiple Myeloma with Extensive Intra- and Extramedullary Disease. J Nucl Med. 2016;57(2):248-51.

Appendix 8: Hyafil F*, Pelisek J, Laitinen I, Schottelius M, Mohring M, Döring Y, Van der Vorst E, Kallmayer M, Steiger K, **Poschenrieder A**, et al., Imaging the cytokine receptor CXCR4 in atherosclerotic plaques with the radiotracer [^{68}Ga]pentixafor for positron emission tomography. J. Nucl. Med. 2017;58(3):499-506. **Highlighted on cover**